



# **Models of Sub-Components and Validation for the IEA SHC Task 44 / HPP Annex 38 Part D: Ground Heat Exchangers**

**A technical report of subtask C  
Report C2 Part D – **Final Draft Revised****

**Date: 16 October 2013**

**By Fabian Ochs<sup>1</sup>, Dani Carbonell<sup>2,3</sup>, and Michel Haller<sup>3</sup>,  
with contributions from Daniel Pahud<sup>4</sup> and Peter Pärtsch<sup>5</sup>**

<sup>1</sup>University of Innsbruck, Unit for Energy Efficient Buildings, Technikerstr. 13,  
A-6020 Innsbruck Austria

<sup>2</sup>RDmes Technologies S.L., Crta N-150, km14.5, IPCT 08227 Terrassa, Spain

<sup>3</sup>Institut für Solartechnik SPF, Hochschule für Technik HSR, Oberseestr. 10,  
CH-8640 Rapperswil, Switzerland

<sup>4</sup>SUPSI, Campus Trevano, CH - 6952 Canobbio, Switzerland

<sup>5</sup>Institut für Solarenergieforschung Hameln GmbH, Am Ohrberg 1, 31860 Emmerthal,  
Germany



## IEA Solar Heating and Cooling Programme

The *International Energy Agency* (IEA) is an autonomous body within the framework of the Organization for Economic Co-operation and Development (OECD) based in Paris. Established in 1974 after the first “oil shock,” the IEA is committed to carrying out a comprehensive program of energy cooperation among its members and the Commission of the European Communities.

The IEA provides a legal framework, through IEA Implementing Agreements such as the *Solar Heating and Cooling Agreement*, for international collaboration in energy technology research and development (R&D) and deployment. This IEA experience has proved that such collaboration contributes significantly to faster technological progress, while reducing costs; to eliminating technological risks and duplication of efforts; and to creating numerous other benefits, such as swifter expansion of the knowledge base and easier harmonization of standards.

The *Solar Heating and Cooling Programme* was one of the first IEA Implementing Agreements to be established. Since 1977, its members have been collaborating to advance active solar and passive solar and their application in buildings and other areas, such as agriculture and industry. Current members are:

Australia	Finland	Singapore
Austria	France	South Africa
Belgium	Italy	Spain
Canada	Mexico	Sweden
Denmark	Netherlands	Switzerland
European Commission	Norway	United States
Germany	Portugal	

A total of 49 Tasks have been initiated, 35 of which have been completed. Each Task is managed by an Operating Agent from one of the participating countries. Overall control of the program rests with an Executive Committee comprised of one representative from each contracting party to the Implementing Agreement. In addition to the Task work, a number of special activities—Memorandum of Understanding with solar thermal trade organizations, statistics collection and analysis, conferences and workshops—have been undertaken.

Visit the Solar Heating and Cooling Programme website - [www.iea-shc.org](http://www.iea-shc.org) - to find more publications and to learn about the SHC Programme.

## Current Tasks & Working Group:

Task 36	<i>Solar Resource Knowledge Management</i>
Task 39	<i>Polymeric Materials for Solar Thermal Applications</i>
Task 40	<i>Towards Net Zero Energy Solar Buildings</i>
Task 41	<i>Solar Energy and Architecture</i>
Task 42	<i>Compact Thermal Energy Storage</i>
Task 43	<i>Solar Rating and Certification Procedures</i>
Task 44	<i>Solar and Heat Pump Systems</i>
Task 45	<i>Large Systems: Solar Heating/Cooling Systems, Seasonal Storages, Heat Pumps</i>
Task 46	<i>Solar Resource Assessment and Forecasting</i>
Task 47	<i>Renovation of Non-Residential Buildings Towards Sustainable Standards</i>
Task 48	<i>Quality Assurance and Support Measures for Solar Cooling</i>
Task 49	<i>Solar Process Heat for Production and Advanced Applications</i>

## Completed Tasks:

Task 1	<i>Investigation of the Performance of Solar Heating and Cooling Systems</i>
Task 2	<i>Coordination of Solar Heating and Cooling R&amp;D</i>
Task 3	<i>Performance Testing of Solar Collectors</i>
Task 4	<i>Development of an Insolation Handbook and Instrument Package</i>
Task 5	<i>Use of Existing Meteorological Information for Solar Energy Application</i>
Task 6	<i>Performance of Solar Systems Using Evacuated Collectors</i>
Task 7	<i>Central Solar Heating Plants with Seasonal Storage</i>
Task 8	<i>Passive and Hybrid Solar Low Energy Buildings</i>
Task 9	<i>Solar Radiation and Pyranometry Studies</i>
Task 10	<i>Solar Materials R&amp;D</i>
Task 11	<i>Passive and Hybrid Solar Commercial Buildings</i>
Task 12	<i>Building Energy Analysis and Design Tools for Solar Applications</i>
Task 13	<i>Advanced Solar Low Energy Buildings</i>
Task 14	<i>Advanced Active Solar Energy Systems</i>
Task 16	<i>Photovoltaics in Buildings</i>
Task 17	<i>Measuring and Modeling Spectral Radiation</i>
Task 18	<i>Advanced Glazing and Associated Materials for Solar and Building Applications</i>
Task 19	<i>Solar Air Systems</i>
Task 20	<i>Solar Energy in Building Renovation</i>
Task 21	<i>Daylight in Buildings</i>
Task 22	<i>Building Energy Analysis Tools</i>
Task 23	<i>Optimization of Solar Energy Use in Large Buildings</i>
Task 24	<i>Solar Procurement</i>
Task 25	<i>Solar Assisted Air Conditioning of Buildings</i>
Task 26	<i>Solar Combisystems</i>
Task 27	<i>Performance of Solar Facade Components</i>
Task 28	<i>Solar Sustainable Housing</i>
Task 29	<i>Solar Crop Drying</i>
Task 31	<i>Daylighting Buildings in the 21st Century</i>
Task 32	<i>Advanced Storage Concepts for Solar and Low Energy Buildings</i>
Task 33	<i>Solar Heat for Industrial Processes</i>
Task 34	<i>Testing and Validation of Building Energy Simulation Tools</i>
Task 35	<i>PV/Thermal Solar Systems</i>
Task 37	<i>Advanced Housing Renovation with Solar &amp; Conservation</i>
Task 38	<i>Solar Thermal Cooling and Air Conditioning</i>

## Completed Working Groups:

*CSHPSS; ISOLDE; Materials in Solar Thermal Collectors; Evaluation of Task 13 Houses; Daylight Research*



## IEA Heat Pump Programme

This project was carried out within the Solar Heating and Cooling Programme and also within the *Heat Pump Programme*, HPP which is an Implementing agreement within the International Energy Agency, IEA. This project is called Task 44 in the *Solar Heating and Cooling Programme* and Annex 38 in the *Heat pump Programme*.

The Implementing Agreement for a Programme of Research, Development, Demonstration and Promotion of Heat Pumping Technologies (IA) forms the legal basis for the IEA Heat Pump Programme. Signatories of the IA are either governments or organizations designated by their respective governments to conduct programmes in the field of energy conservation.

Under the IA collaborative tasks or “Annexes” in the field of heat pumps are undertaken. These tasks are conducted on a cost-sharing and/or task-sharing basis by the participating countries. An Annex is in general coordinated by one country which acts as the Operating Agent (manager). Annexes have specific topics and work plans and operate for a specified period, usually several years. The objectives vary from information exchange to the development and implementation of technology. This report presents the results of one Annex. The Programme is governed by an Executive Committee, which monitors existing projects and identifies new areas where collaborative effort may be beneficial.

### *The IEA Heat Pump Centre*

A central role within the IEA Heat Pump Programme is played by the IEA Heat Pump Centre (HPC). Consistent with the overall objective of the IA the HPC seeks to advance and disseminate knowledge about heat pumps, and promote their use wherever appropriate. Activities of the HPC include the production of a quarterly newsletter and the webpage, the organization of workshops, an inquiry service and a promotion programme. The HPC also publishes selected results from other Annexes, and this publication is one result of this activity.

For further information about the IEA Heat Pump Programme and for inquiries on heat pump issues in general contact the IEA Heat Pump Centre at the following address:

IEA Heat Pump Centre  
Box 857  
SE-501 15 BORÅS  
Sweden  
Phone: +46 10 16 55 12  
Fax: +46 33 13 19 79

Visit the Heat Pump Programme website - <http://www.heatpumpcentre.org/> - to find more publications and to learn about the HPP Programme.

**Legal Notice** Neither the IEA Heat Pump Centre nor the SHC Programme nor any person acting on their behalf: (a) makes any warranty or representation, express or implied, with respect to the information contained in this report; or (b) assumes liabilities with respect to the use of, or damages, resulting from the use of this information. Reference herein to any specific commercial product, process, or service by trade name, trademark, manufacturer, or otherwise, does not necessarily constitute or imply its endorsement recommendation or favouring. The views and opinions of authors expressed herein do not necessarily state or reflect those of the IEA Programmes, or any of its employees. The information herein is presented in the authors’ own words.

## Contents

1	Introduction .....	1
2	Vertical Ground Heat Exchanger Models.....	4
2.1	Analytical far field models.....	5
2.2	Numerical simulations of the ground .....	5
2.3	Models based on g-Functions .....	6
2.4	Borehole thermal resistance models .....	9
2.5	Reference models used in the research field.....	10
3	Horizontal Ground Heat Exchangers .....	12
3.1	General models for Earth to Air Heat Exchangers .....	14
3.2	General models for Shallow GHX.....	15
4	The combination of GHX with solar thermal systems.....	17
5	Model validation .....	18
5.1	Comparison of analytical and numerical g-functions.....	18
5.2	CARNOT EWS model .....	19
5.3	Case Study: Passive House with building integrated HGHX.....	25
5.4	The top boundary of HGHX.....	27
5.5	Short-term model validation and optimisation in TRNSYS.....	29
	Bibliography .....	32
	Appendix A – GHX Models Table .....	36

# 1 Introduction

The American Society of Heating, Refrigerating and Air-Conditioning Engineers (ASHRAE) established a standard nomenclature for ground source heat pumps (GSHP). According to this nomenclature that is described in Kavanaugh and Rafferty (1997), GSHPs can be divided in groundwater heat pumps (GWHPs), surface water heat pumps (SWHPs) and ground-coupled heat pumps (GCHPs). GCHP systems can have open loops using the ground with air as a heat carrier or a water reservoir as a direct energy source. In closed loop indirect systems, a ground heat exchanger (GHX) is linked to a water/brine source heat pump. Direct expansion (DX) closed loop systems are those in which the refrigerant of the heat pump circulates directly through the ground coil. For the purpose of the IEA SHC Task44 / HPP Annex 38, only the GCHP indirect systems will be addressed in this report.

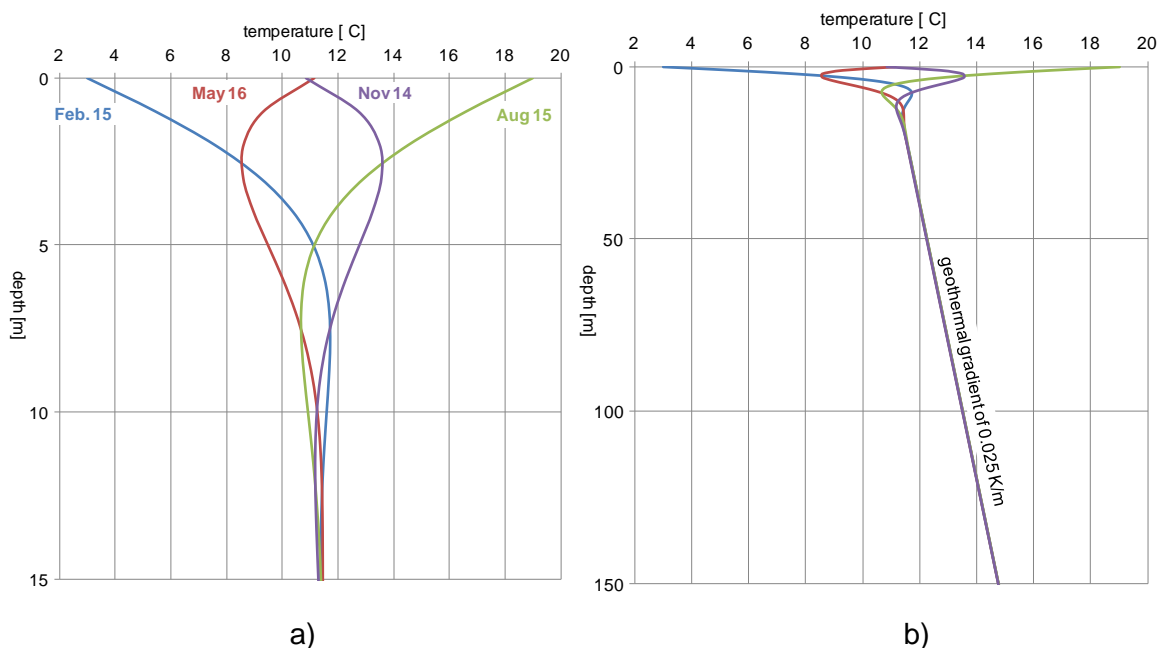


Figure 1: Ground temperature development as a function of the depth and time of the year for shallow depths (left) and medium depths (right).

GCHP systems are growing in a worldwide level, especially in Europe, and Northern America due to its high potential of energy savings and CO<sub>2</sub> emissions reduction. The reason of the better performance of GCHP systems compared to an air source heat pump (ASHP) and conventional fossil fuelled systems can be explained from the soil characteristics. The undisturbed ground temperature as a function of depth derived from the analytical equation of the heat conduction is shown in Figure 1. The undisturbed temperature in the ground from 6 to 100 meters depth is usually close to the mean annual surface temperature at the specific location. Therefore, the ground temperature at some depth is warmer than ambient air in winter, cooler in summer and much more constant over the year providing a better source of energy for the heat pump. Besides these, GCHP systems are able to maintain the performance during peaks loads when ambient air is at extreme conditions (the worst scenario for ASHP). The performance of GCHP may be around 20-30% higher than that of an equivalent ASHP system with seasonal performance factors around 3 to 4 depending of

technology employed and building. It is expected that combining these systems with the solar thermal technology a better performance can be achieved.

In GCHP systems, the heat pump and the GHX are not exposed to outdoor conditions, the compressor has less mechanical and thermal stress compared to ASHP due to the more stable source temperature. Moreover, the evaporator coil does not suffer from frosting avoiding defrosting cycling losses. Thereby, the reliability is higher compared to ASHP with life expectancy of about 20 to 25 years. The ground coils made of polyethylene or polybutylene have higher life expectancy with warranties up to 50 years.

Ground heat exchangers can be classified in horizontal and vertical (HGHX and VGHX) as a function of their physical extension that determines also the depth at which the heat exchange takes place. Examples of both configurations are presented in Fig.1.2. Usually, VGHX have better efficiency and need less land area and pumping energy due to the better thermal characteristics of the soil at deep depth. However, the HGXH are easy and cheaper to install because they are placed at shallow depths. Because of the smaller land area used compared to HGXH, the VGHX are more suitable for large systems.

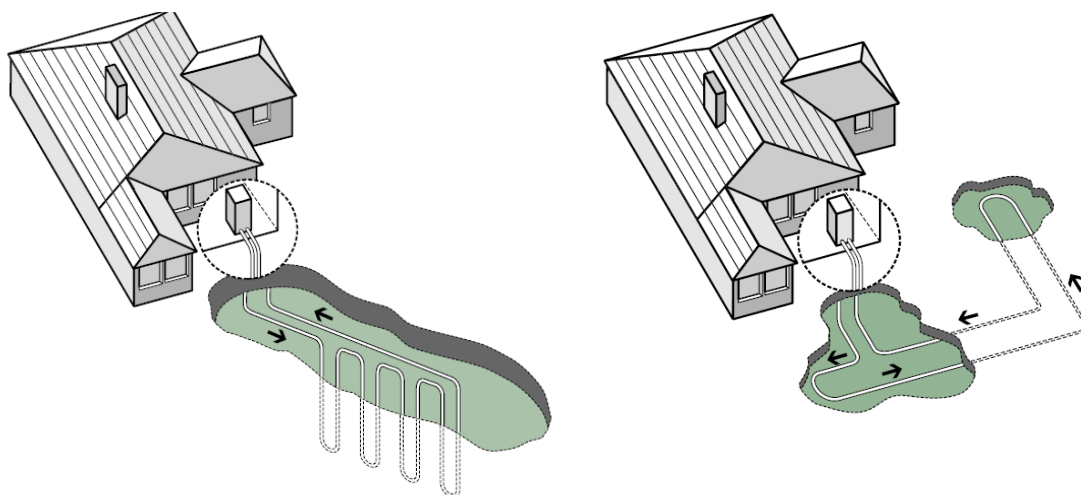


Figure 2: Example of a) a Vertical Ground Heat Exchanger and b) a Horizontal Ground Heat Exchange, CANMET (2002).

The initial capital cost of a GSHP system compared to an ASHP system is around 30 to 40 % higher due to the cost of drilling the borehole and installing the ground coil. Historically, the length of the borehole has been oversized increasing the initial capital and possibly also the operating costs. It is thought that this initial cost is an important barrier for this technology to spread out faster. Therefore, there is a need to have robust models able to size and predict the behaviour of the GHX with precision.

In order to design the system it is mandatory that the loads of the building to be heated or cooled are provided. With this data, the main parameter that all GHX models must calculate is the outlet fluid temperature of the fluid carrier that goes to the heat pump. The minimum or maximum outlet temperatures over the year are typically used to design the length of the GHX considering the capabilities of the heat pump used. For this purpose, the models should consider the effect of the ground properties, soil temperatures distributions and short/long effects due to heat extraction/injection. As a difference from other devices such as the heat

pump, for instance, the GHX is not only sized based on the maximum power of heat or cold delivery, but also based on the total annual energy demand. For design and analysis of GHX for heating/cooling systems, it is often required to simulate the system during several years to get an accurate prediction of the system performance at long term, since each year performance is influenced by the heat exchange resulting from previous years. Thus, the computation time needed for the simulation of these systems is a crucial issue that makes it inconvenient to use three dimensional detailed models with a dense discretization mesh. Therefore, the main focus of the community is on simulation models that deliver annual prediction results within the time frame of minutes to tens of minutes.

One of the main uncertainties in the modelling of GHX is the knowledge of the ground properties, ground water flow and building loads (Yang et.al. 2010). The soil conductivity and borehole effective resistance have a large effect on the predictions of the models. In order to obtain the in-situ values of the soil conductivity and borehole resistance a thermal response test can be used (see for example Gehlin and Hellström, 2003). Obviously, this is a costly process in terms of money that is only used for relatively large systems were the cost of the response test is low compared to the global cost of the installation.

The basic equation for solving GHX is the heat conduction transfer equation described in cylindrical coordinates assuming axial symmetry and homogeneous ground as:

$$\text{Eq. 1} \quad \frac{1}{\alpha} \cdot \frac{\partial T}{\partial t} = \frac{\partial^2 T}{\partial r^2} + \frac{1}{r} \cdot \frac{\partial T}{\partial r} + \frac{\partial^2 T}{\partial z^2}$$

Where  $r$  is the radius,  $t$  is the time,  $T$  is the temperature,  $z$  is the axial distance, and  $\alpha$  is the thermal diffusivity.

One fundamental difference between modelling VGHX and HGHX is the influence of seasonal temperature variations at the ground's surface that affects considerably the performance of HGHX but can be neglected for most VGHX. Consequently, the model's simplifying assumptions to describe the behaviour of the GHX differ quite substantially between VGHX and HGHX and therefore are discussed in different sections.

## 2 Vertical Ground Heat Exchanger Models

Sizing of boreholes is often based on rules of thumb that have been based on simulation results as well as on practical experience. According to VDI 4640 Part 2, the specific heat extraction as shown in Table 1 can be expected for vertical ground heat exchangers. Based on this data, an annual energy extraction ranging from 45 -150 kWh/(m-a) depending on the soil type and operating hours can be assumed.

Table 1: Specific heat extraction in Watt per meter of installed length for VGHX (source: VDI 4640 Part 2, operating hours, valid for sole heat extraction, small systems).

Ground type	Yearly operating hours	
	1800 h/year	2400 h/year
Poor underground $\lambda < 1.5 \text{ W/(m K)}$	25 W/m	20 W/m
Normal underground $1.5 \text{ W/(m K)} > \lambda > 3.0 \text{ W/(m K)}$	60 W/m	50 W/m
Rock $\lambda > 3.0 \text{ W/(m K)}$	84 W/m	70 W/m

Another simple approach explained in CANMET 2002, calculates the length of the GHX for cooling conditions as:

$$\text{Eq. 2 } L_{hx} = 0.051 [K \cdot m/MJ] \cdot \frac{Q_{rej}}{T_{in,max} - T_g}$$

where  $Q_{rej}$  is the energy rejected to the ground,  $T_{in,max}$  is the maximum desired entering temperature in the heat pump, and  $T_g$  is the undisturbed ground temperature. For heating conditions the expression reads:

$$\text{Eq. 3 } L_{hx} = 0.055 [K \cdot m/MJ] \cdot \frac{Q_{abs}}{T_g - T_{in,min}}$$

where  $Q_{abs}$  is the energy absorbed from the ground and  $T_{in,min}$  is the minimum desired entering temperature in the heat pump. The maximum of the two calculated lengths from Eq. 2 and Eq. 3 is used for sizing.

The simpler models showed above should only be used to obtain a rough estimate and should be avoided for sizing the actual borehole length. A recommended approach consists in sizing the GHX by means of computational models are the ones explained in the following.

In order to analyse VGHX's a common approach for reducing calculation time is to split the calculation into a far field problem and a near field problem. The near field, the borehole and its close surroundings, is affected by short term changes in heat extraction as well as by heat transfer between the upward and downward flowing fluid and may be solved on a small time step basis from minutes to hours. The far field problem determines the temperature at the outer boundary of the near field after a certain amount of time (time steps of days or even months) and it depends on axial effects and thermal interference between boreholes (Lamarche et.al., 2007). A review of some of these models can be found in Yang et.al. (2010).

Specific software for geothermal needs are Feflow, Shemat, Plaxis, FRACTure, ModEW, TRAIKON-3D, EWS, BSM, DST, EED, and PILESIM2.

In the following sections different approaches for modelling VGHX are explained.

## 2.1 Analytical far field models

Analytical models are easy to use and very efficient in terms of computational time. However, the configuration and the number of different materials present in the borehole or ground layers with different properties complicate the task of deriving an appropriate analytical model. For this reason, most analytical solutions are based on simplifications such as homogeneous ground properties, axial-symmetry and constant heat flux at the borehole boundary along the length. Analytical models may produce results with less computation time than detailed space discretized methods and are more flexible than tabulated values for given boundary conditions since any configuration can be obtained on the fly. Three main approaches can be found in the literature: the Cylindrical Heat Source model (CHS), the Infinite Line Source model (ILS), and the Finite Line Source model (FLS).

The CHS model considers the borehole as a cylindrical heat source surrounded by an infinite conductive medium. The analytical radial solution for the CHS obtained under constant temperature or heat flux at the cylinder's surface had been presented by Carslaw and Jaeger (1947). An extended sizing model based on this approach was derived by Kavanaugh and Rafferty (1997).

The ILS model for VGHX was described by Ingersoll et.al. (1954) based on Kelvin's line source theory. This model assumes that the borehole is an infinitely long line submitted to a constant heat flux per unit length. The use of the ILS model for design purposes is described in the International Ground-Source Heat Pump Association manual (IGSHPA, 1988).

In contrast to the ILS and CHS models, the FLS model account for the fact that the borehole has a finite length considering the axial effects. The use of a FLS model for the simulation of VGHX was proposed by Claesson and Eskilson (1987) using the temperature at the medium of the borehole length. The proposed analytical solutions were later modified by Zeng et al. (2002) using the average temperature of the borehole and finally numerically solved by Lamarche and Beauchamp (2007).

Most of the analytical models present in the literature are not suitable for short term analysis since the thermal capacity of the borehole is not accounted for. Only recently some studies have addressed this issue within the framework of the analytical models (see Lamarche and Beauchamp 2007 and Saqib and Claesson 2011).

## 2.2 Numerical simulations of the ground

Numerical models existing in the literature are mainly based on discretization techniques on finite volumes. They are computationally more demanding than analytical models but they are more versatile in the sense that they can be used for inhomogeneous grounds, the influence of ground water flow and near field problems such as the short time responses inside and in the vicinity of the boreholes can be considered. For the influence of the heat extraction on the far field however, the latter effects are not of importance. In the literature many numerical models have been presented. The work conducted at Lund University has been used as a reference for many years (Claesson and Eskilson, 1987; Eskilson, 1987; Hellstrom, 1991). Numerical simulations of the ground are quite often combined with

borehole thermal resistance models to include the short term effects in the borehole itself and between the upstreaming and downstreaming fluid in the pipes, or with the g-function approach for the determination of the time dependent temperature at a certain distance from the borehole.

Pure numerical models are solving all the physical domain using two or three dimensional discretization by means of finite volume (FVM) or finite elements methods (FEM). Figure 3 shows an unstructured mesh of a borehole with a single U-pipe and some of the surrounding earth. Typically, only the conductive part is solved and only in very few cases the fluid part by means of Computational Fluid Dynamics (CFD) models are solved. Instead, proper boundary conditions at the pipe walls are imposed. Examples of these models can be found in Muraya et.al. (1996), Li and Zheng (2009), Bauer et.al. (2012), and Lamarche et.al. (2010). These models are quite computationally intensive and are therefore usually not suited for yearly energy simulations without further simplifications.

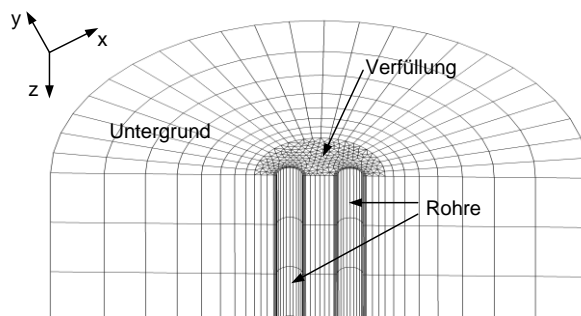


Figure 3: Discretization mesh in a detailed 3D model. Source: Bauer (2012).

General commercial software for solving conductive and/or convective problems using FVM or FEM are, for example, ANSYS, Fluent, Heat3, Comsol, STARCD, Abaqus or the open source software Open Foam.

## 2.3 Models based on g-Functions

A popular approach for the determination of the temperature at a given distance of the borehole after a certain time consists in using the g-functions proposed by Eskilson (1987). The g-functions are defined as the non-dimensional thermal response factors of the borehole field. They can be derived from analytical solutions or from numerical simulations using discretization methods of the differential heat conduction equation.

### 2.3.1 Long term and midterm application of g-functions

The non-dimensional thermal response factors depend on two parameters:  $t/t_s$ , the dimensionless time (time divided by the time constant  $t_s = H^2 / (9 \cdot \alpha_g)$  of the borehole, being  $H$  the borehole length and  $\alpha_g$  the thermal diffusivity of the ground, and  $r_b/H$ , the ratio of borehole radius  $r_b$  to borehole length  $H$ .

Once a g-Function is known, the temperature difference between the outer margin of the borehole  $T_b$  and the undisturbed ground  $T_g$  can be calculated knowing the thermal conductivity of the ground  $\lambda_g$  and the constant heat extraction rate  $\dot{q}_{GHX}$  by:

$$\text{Eq. 4} \quad T_b - T_g = g \left( \frac{t}{t_s}, \frac{r_b}{H} \right) \cdot \frac{\dot{q}_{GHX}}{2\pi\lambda_g}$$

Although Claesson and Eskilson (1987) presented an analytical solution of the FLS theory, Eskilson (1987) used a detailed multi-dimensional simulation model (the SBM model) for the determination of the g-functions, including also the temperature response of multiple boreholes. These functions were stored in a data base in order to avoid expensive computations every time a calculation is performed. This implies a lack of flexibility because g-functions need to be pre-calculated for each configuration and a new configuration cannot be solved without this pre-processing task. The analytical solutions of the g-functions using the FLS method are a very efficient way to overcome this problem.

As an illustrative example, a comparison of the g-functions for a single borehole submitted to a constant heat extraction rate of 1 W/m with the three main analytical models described above are presented in Figure 4. It can be observed that the CHS and the ILS predictions never reach a steady state, thereby not describing the physical behaviour of the borehole at long term. Predictions for medium term are very similar for all the models. Discrepancies between them appear at around  $\ln(t/t_s) = -4$ , where axial effects become important. This corresponds to 9 months if one assumes a borehole length of 100m with a soil diffusivity of 0.078 m<sup>2</sup>/day. Therefore, the assumption of infinite length may not be a problem for midterm estimations, but it may lead to an underestimation of the performance of the ground heat exchanger in the case of long term heat extraction (heating), and to an overestimation of the performance in the case of long term net heat injection (cooling).

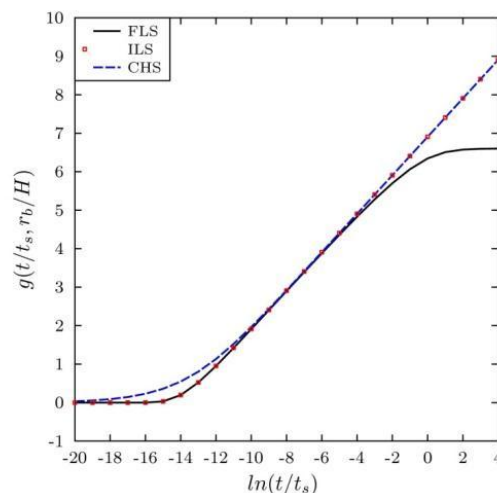


Figure 4: Comparison between the g-function calculated with the analytical models. Finite Line Source (FLS), Infinite Line Source (ILS) and Cylindrical Heat Source (CHS). Source: D. Carbonell.

A single g-Function may be used to determine the temperature drop at the borehole wall after one or more years which is important for the estimation of the long term deterioration (or improvement in the case of solar heat input) of VGHXs. In the case of solar ground recharging the average net annual heat extraction is used for  $\dot{q}_{GHX}$ , which is a negative value if

more heat is extracted than re-charged, but can be a positive value in the case of excessive charging by solar energy.

For the prediction of medium term response of the borehole in the range of weeks, the temporal superposition of a series of g-functions is used, e.g. by superimposing constant heat extraction/rejection fluxes as a series of step pulses as shown in Eq. 5:

$$\text{Eq. 5} \quad T_b(t) = T_g + \sum_{i=1}^n \frac{(q_i - q_{i-1})}{2\pi\lambda} \cdot g\left(\frac{t_n - t_{i-1}}{t_s}, \frac{r_b}{H}\right)$$

The modelling of a number of boreholes which interact with each other can be achieved with a spatial superposition of g-Functions. This concept assumes that the average temperature is the sum of all contributions from all boreholes (N).

$$\text{Eq. 6} \quad T(r, z, t) = \sum_{i=1}^N T_i(r_i, z_i, t)$$

As state before, g-functions are derived for medium and long term analysis. Eskilson (1987) estimated the time of  $5r_b^2 / \alpha_g$  above the value of which the model assumptions were valid. For a borehole of radius of 5 cm and soil diffusivity of  $0.078 [m^2 / day]$  this time correspond to 3.8 hours. For most typical soils and boreholes, this time range between 3 and 6 hours (Yavuzturk et.al., 1999).

The g-functions approach has been extensively used for sizing borehole fields. For example, the well-known commercial standalone software EED-Earth Energy Designer (Hellstrom et.al., 1997) and GLHEPRO (Spitler, 2000) are based on this method.

### 2.3.2 Extension of g-function models to near field problems for short time simulations

There is a general view that short time effects are important, not only to model hourly loads, but to reduce the predicted length of the boreholes that may be oversized if short effects are not considered. The thermal capacity of the borehole is not as high as the ground capacity and thereby the effects of heat extraction/injection rates affect the borehole response at short time scales. Solving this time scales area also important in order to consider heat pumps cycling losses.

The short time g-function model presented by Yavuzturk et.al. (1999) is an evolution of Eskilson's work. The borehole is solved by means of axial-symmetric finite volume discretization including the capacitance of the borehole, i.e pipe and grout, which were previously neglected by Eskilson. The discretized mesh is structured and therefore a pie-sector approach is used in order to account for pipes configuration. The results of the numerical model were expressed in terms of g-functions, which allow for the use of the same implementation in a system simulation algorithm as for long term g-functions. This short time g-functions are nearly the same as the ones proposed by Eskilson for medium and large term. In the present case, however, the g-function is redefined as:

$$\text{Eq. 7} \quad g\left(\frac{t}{t_s}, \frac{r_b}{H}\right) = \frac{2\pi\lambda}{q} (T_b - R_b q - T_g)$$

Where  $R_b$  is the borehole thermal resistance. When short time g-functions are used in yearly simulation calculations with hourly loads, the calculation time is very large. For this reason several aggregation schemes have been proposed (Yavuzturk et.al., 1999; Bernier et.al., 2004; Marcotte & Pasquier 2008). These schemes are based on the idea that not all load

history is of importance, but only after certain time ago. Using this hypothesis, older loads can be lumped to larger blocks while preserving newer loads to keep the short-time information.

Recently a very promising model has been developed by Claesson & Javed (2011). This model is able to solve efficiently the time scales from minutes to years. This model is based on the analytical solution of the borehole including the thermal capacity of the fluid and grout (Javed & Claesson, 2011).

## 2.4 Borehole thermal resistance models

For the simulation of GHX, the thermal resistance problems of the borehole interacting with the fluid including the thermal capacity term have to be solved.

The borehole thermal resistance depends on the grout properties, pipes materials, fluid and geometry of the legs. A simple approach consists on solving the problem in a zero-dimensional fashion and considering this resistance as a steady state value. This approximation can be used because the capacity of the borehole is negligible compared to the ground capacity. The three resistance that need to be calculated are the grout resistance, the inside convective resistance between the fluid and the wall pipe and the conductive resistance of the pipe material. The convective and conductive resistance can be calculated by typical expressions found in many books and will not be addressed here.

The main problem relies in how to calculate the thermal resistance of the grout.

Bennet et.al. (1987) proposed the multipole method. This model seems to be the most accurate method for calculating the thermal resistance of the grout (see Lamarche et.al. 2010), and is used in EED (Hellström, 1997), and GLHEPRO (Spitler, 2000).

A simplification of this method, the so-called line-source formulae, was proposed by Hellström (1991), where several analytical expressions for particular configuration were described. The line source formulae method with the parameters  $R_a$  and  $R_b$  is used in the DST model and also in TRNSBM and EWS.

However, these methods use quite complex equations. Alternatively, for a single U-pipe, the grout resistance can be easily obtained from:

$$\text{Eq. 8} \quad R_{grout} = \frac{1}{\lambda_{grout} \cdot \beta_0 \cdot \left( D_{bore} / D_{pipe} \right)^{\beta_1}}$$

Where the terms  $\beta_0$  and  $\beta_1$  are calculated as a function of the shank spacing obtained from experimental fits by Paul (1996). Another equation fit obtained from numerical simulations was proposed by Sharqawy et.al. (2009).

All above methods assume a two-dimensional analysis, but the effects of downwards and upwards different fluid temperatures in the resistance cannot be accounted for with only two-dimensions. For this reason quasi-three dimensional models have been proposed to account for the axial effects. Comparisons of some of these models against a fully 3D unstructured finite volume method have been presented recently by Lamarche et.al. (2010).

## 2.5 Reference models used in the research field

### 2.5.1 The superposition borehole model (SBM) and TRNSBM

The Superposition Borehole Model (SBM) has been developed by P. Eskilson at the Lund Institute of Technology (LTH), Sweden, in order to provide a tool for the analysis and design of multiple borehole heat exchangers' systems (Eskilson 1986, 1987). The SBM model has been implemented into TRNSYS by Pahud et al. (1996) at the EPFL in Lausanne. It enabled the use of the model for the analysis and optimization of a borehole field as part of a complete thermal energy system. The TRNSYS implementation included the concept of effective borehole thermal resistance described by Hellström (1991). The two thermal resistances that determine the borehole heat transfer characteristics (Hellström's  $R_a$  and  $R_b$ ) may either be constant values or read in from a file to reflect a flow- and temperature-dependent behaviour. This version of TRNSBM has been adapted to TRNSYS 16 or 17 by Pahud (2012) at SUPSI in Lugano. It corresponds to the original branch of SBM model for TRNSYS. Another branch was created in 1997 by TRANSSOLAR. It further developed the TRNSYS version from 1996 to include multi-ground layers, but lost the ability to simulate inclined boreholes.

The model (Pahud 2012) calculates the three-dimensional temperature field in the ground for a system with an arbitrary number of vertical or inclined boreholes. The heat flow problem, assumed to occur by pure heat conduction in the ground, is solved by using the explicit forward differences (FDM). The steep temperature gradients close to the boreholes and the complicated three-dimensional geometry in the ground are solved by taking advantage of all the inherent symmetries of the process and using the superposition technique. In each borehole, the upward and downward fluid temperatures vary along the pipes and with time. The convective heat flow in the pipes is balanced against the conductive heat flows between the pipes and the borehole wall. The heat balance equations in the boreholes are solved for the steady-state case. The short-time capacitive effects due to the rapid variation of the loading conditions can successfully be taken into account by adding a "pipe" component in the TRNSYS simulation environment (see chapter 5.5). The hydraulic coupling between the boreholes can be arranged in many different ways, allowing for the combination of series and parallel coupling of the boreholes. They may also be coupled in separate hydraulic systems, i.e. each with independent inlet fluid temperatures and flow rates. The air temperature on ground surface is also an input and may vary with time. Initial ground temperature is defined with a temperature at the ground surface and a constant geothermal temperature gradient.

Output variables are the transferred heat rate, the outlet fluid temperature and flow rate per hydraulic systems. Energy and temperature summaries, temperature fields in horizontal and vertical planes may optionally be obtained.

### 2.5.2 Duct Storage Model (DST)

The Duct Storage Model (DST) has been developed by Hellström (1991) and it was originally designed for seasonal ground thermal energy storage applications. The boreholes are assumed to be uniformly distributed within a cylindrical shape storage region.

The basic problem in the analysis of duct ground heat storage systems is the interaction between the two main thermal processes. The first consists of the interaction between the ducts and the surrounding ground, the so-called global or macro scale problem, and the second is the local thermal process around the pipes.

The model considers the spatial superposition of two parts plus the steady-flux part around the nearest pipe. The solution of local region accounts for short time responses and is solved using a one dimensional radial discretization mesh. For the global problem, which determines the global losses from the store, is solved by means of two-dimensional axial-symmetric formulations. The steady flux, used to calculate the redistribution of the heat in the storage volume is solved analytically.

The DST model assumes that the heat exchangers are densely packed and equally distributed. These assumption might not be appropriate for cases where the borehole field is used for dissipate and not for store (Yavuzturk and Spitler, 1999). However, when calibrated, this model has shown to perform well (Thornton et.al., 1997), and is considered one of the reference models.

DST model has been implemented as standalone tool and as TRNSYS type. It has the limitation of using always a circular shape with equally distributed boreholes. TRNSYS-DST can account for temperature and flow dependent borehole resistance by pre-processing it using another program called BORE.

### 2.5.3 The EWS model

This model has been developed by Huber & Schuler (1997). The EWS model simulates the earth in a radius of about 2 m around the borehole based on a one dimensional finite difference approach with the Crank-Nicholson algorithm. In its original version, the temperature at the outer boundary of this cylinder is determined by an analytical solution based on the ILS theory. Later on, this part has been replaced by g-Functions of Eskilson and at the same time the model has been extended from single borehole calculation to multiple boreholes (Huber & Pahud 1999). In contrast to many other simulation programs, the EWS allows for the definition of several horizontal ground layers with different properties. The 1D transient algorithm must be solved for each layer. Moreover, in each layer a thermal balance considering the fluid going upwards and downwards is considered.

The EWS can be used as a stand-alone tool that can be obtained from [www.hetag.ch](http://www.hetag.ch). The original version of the EWS model for single boreholes has been implemented in TRNSYS type 451 (Wetter & Huber 1997). The EWS has also been implemented in Simulink (Bianchi 2006) and in Polysun ([www.velasolaris.ch](http://www.velasolaris.ch)) for single boreholes and borehole fields.

### 3 Horizontal Ground Heat Exchangers

The HGXH can be classified in three groups: i) horizontal, ii) vertical and iii) building integrated. Some examples of horizontal orientations are meander, harp, bifilar, capillary pipes and earth to air heat exchangers. Trench, cage and basket/helix are examples of vertical oriented types. Moreover, the HGXH can be integrated in the basement of a building, in the walls or as and energy piles. Illustrative examples of the group i) and ii) are shown in Figure 5.

Examples of building integrated ground heat exchangers are presented in Figure 6. These configurations offer high cost-reduction potential. However, their application is low compared to the other configurations due to the limited capacity and in particular because freezing has to be prevented.

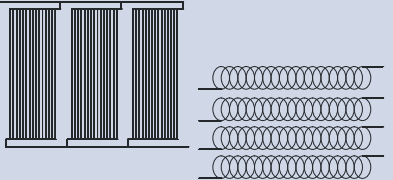
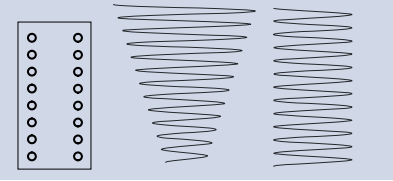
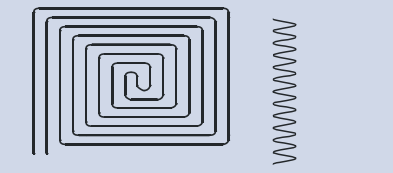
Type	figure	scheme
<b>horizontal ground heat exchanger</b>		
capillary collector meander/harp		
<b>trench heat exchanger</b>		
compact absorber baseket / helix		
<b>building integrated heat exchanger</b>		
energy pile, basement/ wall absorber		

Figure 5: List of some available ground heat exchangers.

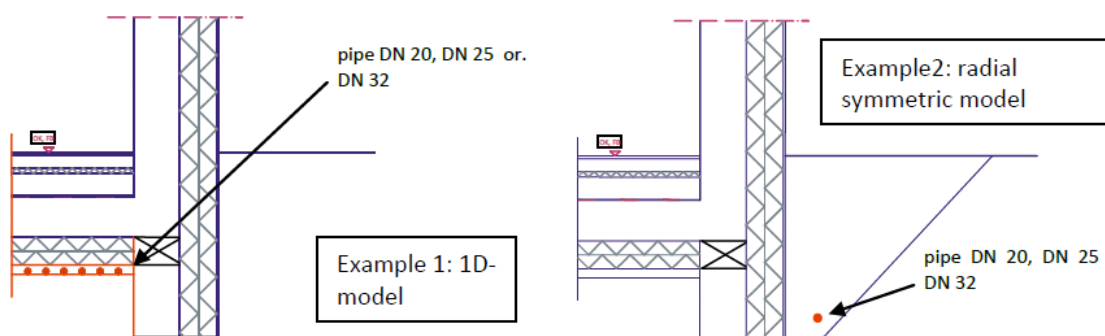


Figure 6: Horizontal ground heat exchanger in blinding layer with 360 m piping in 4 parallel loops (1D model, left) and ground heat exchanger in surrounding excavation with a length of 52 m (right).

Again, the simplest approach to size the GHX consists in using rules of thumb. The expected specific extraction power for small systems presented in Table 2 is given by VDI 4640. Based on this data, an annual energy extraction ranging from 18 –77 kWh/(m<sup>2</sup>a) depending on the soil type can be expected.

Table 2: Specific heat extraction in W/m<sup>2</sup> of installed length for HGHX (source: VDI 4640, valid for only heat extraction and for small systems).

Ground type	Yearly operating hours	
	1800 h/year	2400 h/year
Poor underground $\lambda < 1.5$ W/(m K)	10 W/m <sup>2</sup>	8 W/m <sup>2</sup>
Normal underground 1.5 W/(m K) $> \lambda > 3.0$ W/(m K)	20-30 W/m <sup>2</sup>	16-24 W/m <sup>2</sup>
Rock $\lambda > 3.0$ W/(m K)	40 W/m <sup>2</sup>	32 W/m <sup>2</sup>

Alternatively, the formulas presented in CANMET (2002), for cooling conditions can be used:

$$\text{Eq. 9 } L_{hx} = \frac{CL \left( \frac{COP_c + 1}{COP_c} \right) \cdot (51 + R_s + PLF_c)}{T_{in,max} - T_{max,g}}$$

For dominated heating loads the expression reads:

$$\text{Eq. 10 } L_{hx} = \frac{HL \left( \frac{COP_h + 1}{COP_h} \right) \cdot (51 + R_s + PLF_h)}{T_{min,g} - T_{in,min}}$$

In above expressions,  $CL$  and  $HL$  are the cooling and heating loads,  $COP$  is the coefficient of performance of the heat pump,  $R_s$  the soil/field resistance in [m<sup>2</sup>K/kW] and  $PLF$  the design month's part load factor. The subscripts  $h$  and  $c$  refer to heating and cooling respectively. When heating and cooling are present, the highest length of the result of Eq. 9 and Eq. 10 are used.

The HGHX are characterized for being placed at shallow depths, usually between 1-3 meters. Thereby, they are strongly influenced by weather conditions such as variation of the ambient temperature, thermal radiation (solar and long wave), rain and snow (including thawing). An illustrative example of the phenomena involved in the air to ground interface can be seen in Figure 7 where amb refers to ambient, c to cover, s to surface and gw to ground water.

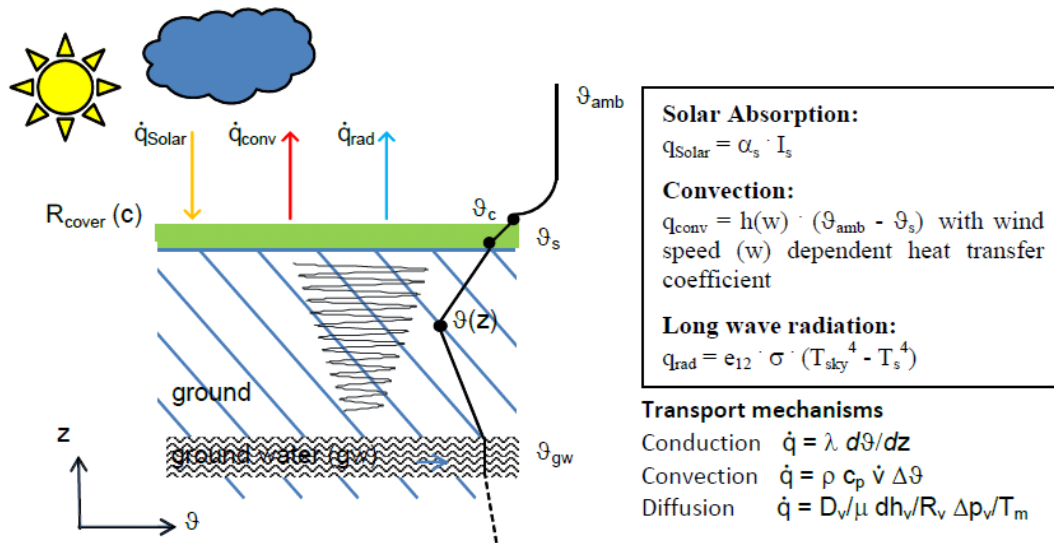


Figure 7: Boundary conditions, heat transfer and temperature profiles in the air ground interface.

In addition to all these processes, freezing of the soil in the vicinity of the pipes may play an important role improving the GHX performance due to the latent heat release, thermal storage and increase of soil thermal conductivity of the frozen region (Mei, 1984). Because of the strong influence of the moisture content on the thermal capacity of the soil, the water diffusive transport equation may also be considered. In the case of air ground heat exchangers, heat transfer due to phase change (evaporation/condensation) has to be taken into account.

Nevertheless, most of the models available in the literature only consider the conductive heat transfer not only because it is the predominant effect (see Ramming 2007 for example) but also because of the added complexity of the other phenomenology and the knowledge uncertainty of some relevant parameters.

Different models for the annual performance simulation of heating/cooling systems have been described in literature. These models are generally divided in two groups mainly depending on the fluid carrier and type of loop: i) open loops with earth to air heat exchangers and ii) closed loops with water/glycol using shallow ground heat exchangers. A review on ground heat exchange models is presented by Florides & Kalogirou (2007).

### 3.1 General models for Earth to Air Heat Exchangers

In order to design and predict the behaviour of an earth to air heat exchanger, the air outlet temperature is the parameter that all the models must calculate. Besides this, the ground temperature distribution and the humidity air content for some applications may also be of interest.

Tzaferis et.al. (1992) analysed eight models for ground air heat exchangers with relatively similar results between them regarding the prediction of the outlet air temperature. Among them, some models were based on analytical solutions while others were derived from numerical technics ranging from one to three dimensions.

Most of the simplified models do not calculate the ground temperature distribution and the humidity air content. For this reason, Mihalakakou et.al. (1994) presented a model based on

an implicit transient 2D finite volume method able to account for this phenomena using a polar discretization around the buried pipe and considering the soil thermal stratification. Afterwards, this model was used in Mihalakakou et.al. (1996) to analyse the heating potential of earth to air heat exchangers of various tubes. The solution for various pipes was obtained by means of superposition techniques. Hollmuller and Lachal (2001) presented a detailed finite difference model able to account for latent heat, frictional losses and water infiltration along the pipe. The model was successfully validated with long-term monitored data in Hollmuller (2002). More recently, a simplified transient analytical model was presented by Cucumo et.al. (2008) using two independent coordinated for the fluid flow direction and for the ground perpendicular to the pipe axes. Although the model simplifications and its analytical approach, the model can include condensation effects and was found to predict satisfactory results.

### 3.2 General models for Shallow GHX

Most of the models before the 90th were based on the line source theory explained in section 2.1 for VGHX. As a consequence, the GHX length was oversized. A more elaborated model was presented by Mei (1986) using a finite volume method, that simulates the ground around the buried pipe by means of a 2D cylindrical discretization. At the boundary of the cylinder, the temperature of the undisturbed ground was obtained as a function of time in the year and depth neglecting the influence of neighbouring pipes.

Some years later, an improved version of Mei's model was presented by Giardina (1995) and implemented in TRNSYS (available as TESS Type 556) using the same hypothesis assumed in the original work. A schematic of the problem solved by Giardina can be seen in Figure 8. The model assumes symmetry and considers the outer boundary of the simulation, the so-called far field radius, to be the temperature of the undisturbed ground calculated as a function of time in the year and depth. Different ground temperatures in the direction of the fluid path are a result of several capacitance nodes in the direction of the pipe / fluid path. However, the resulting difference in the far field radius is neglected in this model, and thus the heat extraction from the ground is somewhat overestimated. The far field radius is further limited by the depth where the pipes are buried. One of the main disadvantages of this model is that the influence of neighbouring pipes is neglected.

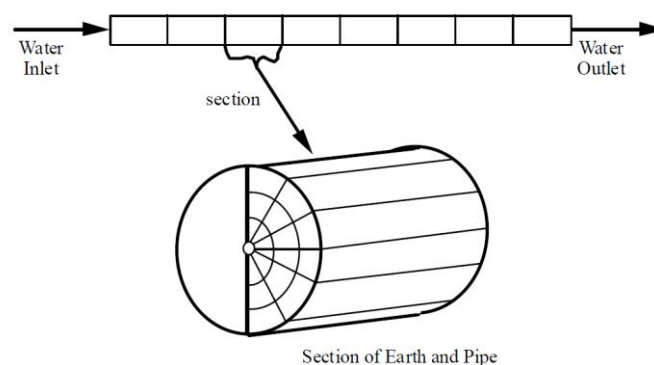


Figure 8: Model discretization of a GHX by Giardina (1995).

Tarnawski and Leong (1993) developed a detailed finite element 2D model able also to consider freezing/thawing and the complexity of the soil surface processes due to the climate

and topographic conditions. Piechowski (1995) also used the Mei's model but considering the moisture transfer in the soil by means of an implicit 2D finite volume method.

Bojic et al. (1997) developed a model in which the soil is divided into horizontal layers with uniform temperature. All the pipes are placed in one layer at the same depth and parallel to each other. The heat transported to the soil by convection from the air and the solar irradiation is calculated.

Ramming (2007) presented a similar methodology employed by Mei, but also including freezing effects. The model reflects time-dependency of ground properties such as moisture, water infiltration, etc... However, the author concludes that the soil properties in 1.5 m depth change only over long time-periods, and therefore constant values can be used for one year. On the top, the simulation boundary is a source/sink according to the assumed heat transport phenomena between the ground and the atmosphere. Ramming's work concluded that ice formation is of relevance for most HGHX whose design and sizing is usually such that return temperatures to the ground may be below 0°C for several weeks in the year and that are usually placed in moist ground. The average moisture of the ground is of importance because it affects the thermal conductivity and heat capacity of the soil. However, the prediction of the transient moisture content evolution in the soil is usually not necessary.

A similar model was presented by Glück (2009). Based on a rough estimation of the influence of precipitation, Glück (2009) argued that the effect of heat input into the ground by precipitation can be neglected, and precipitation is therefore only a factor that affects the water content and thus the heat transfer coefficient and latent energy changes (water/ice) within the ground. In this model the heat exchange with the atmosphere is modeled with a combined heat transfer coefficient (convection and long-wave radiation) towards a solar ambient temperature (see section boundary conditions, below) that includes not only the measured ambient temperature but also the influence of solar irradiation.

Wu et al. (2010) used the commercial CFD software package FLUENT to predict the thermal performance of a portion of the horizontal-coupled slinky and straight heat exchangers. A transient 3D sensible heat transfer model for the ground coupled heat exchanger was used.

All of the methods presented above neglect the effects of neighbouring pipes. An idea to solve the interaction between pipes was proposed by Cauret and Bernier (2006) applying the analytical g-functions, the so called FLS method typically used for VGHX, to solve a new compact collector design.

Recently, Ochs and Feist (2012a) have shown that most configurations, the HGXH can be modelled with analytical models for the fluid flow while the soil can be solved using for example a 1D multi-layer model (see for example D. Carbonell et.al. 2011). Complex geometry's of GHX such as trench, basket collectors or building integrated are more likely to be modelled with 2D (or 3D) formulations. With 2D FE models based on the Matlab PDEtool that have been implemented in Matlab/Simulink using s-functions complex geometries of HGHX can be modelled and freezing can be considered (Ochs 2012b).

## 4 The combination of GHX with solar thermal systems

The use of solar thermal energy may reduce the annual load of GHX and thus the size of the GHX system may be reduced for cases where the annual load or the long term degradation of the temperature in the ground is the size determining factor. However, the size of the GHX system may not be reduced for cases where the short term heat extraction power is the size determining factor since it cannot be expected that the maximum heat extraction power will be affected by the use of solar thermal energy.

For systems with active regeneration of the ground with excess solar thermal energy in summer, attention has to be paid to the fact that severe deterioration of the heat conduction in the borehole / ground may result if the temperatures used for recharging are too high. These effects are usually not considered in simulation models and are left to the proper judgement of the engineer or planner. Recharging of ground heat exchanger systems by solar thermal energy has been reported to reduce the long term temperature deterioration to zero if the heat extraction and heat input are balanced, and to change the sign of the long term temperature response for cases where heat is charged in excess of the extraction. These effects can be simulated both with g-Function approaches as well as with finite difference models. Since the effect of temperature degradation with time is only minor for single boreholes, also the effect that can be achieved with recharging by solar thermal energy is only minor<sup>1</sup>. For borehole fields of limited distance between the single boreholes however, the effect may be significant both for systems with excessive heat extraction and also for systems with surplus charging.

---

<sup>1</sup> However, the effect can play a major role if the inlet temperature of the VGHX falls below the minimum value (like 0 °C in Switzerland) and the electric back-up heating takes over the heat demand in winter. This becomes very relevant for undersized GHX systems for example if the actual heat demand is higher than expected (Bertram et al. 2013).

## 5 Model validation

### 5.1 Comparison of analytical and numerical g-functions

by Dani Carbonell

The Finite Line Source (FLS) model described in Lamarche and Beauchamp (2007) has been implemented and compared to numerical solutions of the g-functions presented by Eskilson (1987).

In order to numerically solve the FLS equations, numerical integration algorithms are necessary. In the present case, the GLE Scientific Library has been used.

Comparisons between the analytical and the numerical g-functions solutions have been performed for two borehole fields. Results are presented in Figure 5.1.1 (left) for two boreholes and in Figure 5.1.1 (right) for an array of eight boreholes in one line. The nomenclature used in Figure 5.1.1 has been explained in section 2.3.

As it can be observed, predictions by the analytical FLS and the numerical model of Eskilson are very similar for all the range. The FLS method is an accurate and robust model that can be used to obtain g-functions of any borehole field on the fly. Therefore it is not necessary to store the g-functions in a library and doing a pre-processing task, the calculations of the borehole field using the FLS model is very fast and can be computed at the beginning of each simulation.

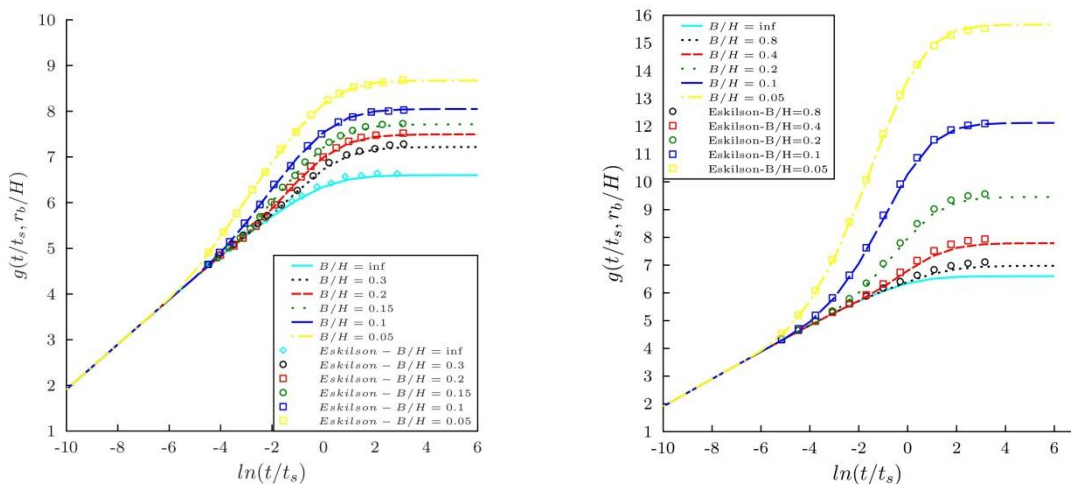


Figure 5.1.1: Comparison between analytical using the FLS (lines) and numerical g-function models (symbols); array of left) two and right) eight boreholes in one line.

## 5.2 CARNOT EWS model

by Fabian Ochs

The CARNOT EWS model is a transient model for dynamic simulation of VGHX in the simulation environment Matlab/Simulink within the CARNOT Blockset.

The model is based on the equations described by Huber (1997) and has been implemented using the state space model of Matlab/Simulink by Bianchi (2006).

The geometric (e.g. depth and diameter of bore or type of borehole heat exchanger) and physical (e.g. ground properties) parameters as well as the operational parameters and boundary conditions are defined in a script (m-file), which is executed before simulation (initialization). Consequently, changes of the mass flow during operation/simulation could not be considered in the original model.

In the majority of cases a ground heat exchanger will be operated with constant mass flow and thus varying mass flow will rarely occur, however, simulation of discontinuous operation (on-off) is certainly required. As the original model did not allow for that the model was enhanced and on-off operation was implemented in the actual version. Furthermore, the originally used "Trichterformel" as boundary condition was changed to a boundary condition based on g-functions (Eskilson, 1987) in order to allow for multiple borehole configurations. The third modification concerns the initial conditions. Whereas in the original model the nodes of the numerical grid were initialized with a homogenous temperature field, in the actual version a temperature distribution based on the steady state solution using g-functions can be calculated.

In the following, the model is briefly described. Finally, different validation calculations have been performed, which will be presented after the description of the model.

The Simulink EWS model was developed by Bianchi (2006) based on the description of the standalone EWS model (Huber and Schuler, 1997). However, some simplifications (single borehole, constant mass flow "= always on") restricted the use of it. The model was improved by the author and validated against measured data of a thermal response test and simulated data of a fully discretized model from Bauer (2012) to test short term behaviour. Furthermore, cross-validation was performed with EED to check long-term behaviour.

### Validation

For the validation three cases have been investigated. The first validation example is measured data from a thermal response test [IEA ECES A21]. The second case is a validation against a fully discretized 3D ground heat exchanger model with simulated data of a period of heat injection from Bauer (2012). Both cases address the short term behaviour. For the validation of the long term behaviour of the ground heat exchanger model the results are compared with numerical results of calculation methods such as EED and EWS (third case).

#### Case 1: Thermal response test

The thermal properties of the grout and the ground are summarized in Table 5.2.1. The borehole properties are listed in Table 5.2.2.

Table 5.2.1 - Thermal properties of grout and ground.

	Grout	Soil
$\lambda$ [W/(m K)]	2.1	2.3
$\rho$ [kg/m <sup>3</sup> ]	2500	2500
$c_p$ [J/(kg K)]	800	800

Table 5.2.2 - Borehole properties and parameters.

Type	2-U
Height	$H = 193$ m
Borehole diameter	$D_b = 0.2$ m
Pipe	$D = 40/3.7$ mm
Mass flow	$\dot{m} = 0.44$ kg/s (water)
Undisturbed ground temperature	$\vartheta_g = 14.7$ °C

The measured and calculated development of the flow temperature (out) for a given inlet temperature (in) is shown in Fig. 5.2.1. The simulation results are shown for the case that the resistances  $R_1$  and  $R_2$  are calculated based on different models. For the latter case the agreement between simulated and measured data is very good.

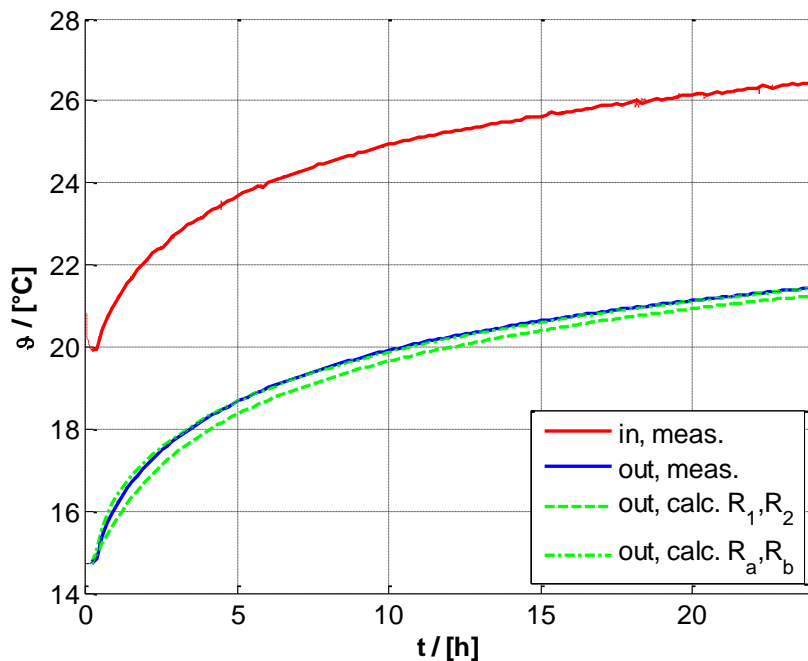


Figure 5.2.1 – Comparison of Simulink EWS model with TRT measurement data (IEA ECES A21).

The maximum deviation with regard to injected heat (integrated injected power) is below 5% even in case of the simulation based on resistances  $R_1$ ,  $R_2$  (see Table 5.2.3).

Table 5.2.3 - Comparison of measurement and simulation based on resistances  $R^1$ ,  $R^2$ .

	Q (90h) [kWh]	Q (24 h) [kWh]
TRT	825.5	436.5
EWS	847.3	455.7
err / [%]	2.7	4.4

### Case 2: ANSYS FEM Simulation

The thermal properties of the grout and the ground are summarized in Table 5.2.4. The borehole properties are listed in Table 5.2.5.

Table 5.2.4 - Thermal properties of grout and ground.

	Grout	Soil
$\lambda$ [W/(m K)]	2.3	2.2
$\rho$ [kg/m <sup>3</sup> ]	1460	2600
$c_p$ [J/(kg K)]	1500	850

Table 5.2.5: Borehole properties and parameters.

Type	2-U
Height	$H = 100$ m
Borehole diameter	$D_b = 0.13$ m
Pipe	$D = 32/3.0$ mm
Pipe distance	$B_u = 0.06$ m
Mass flow	$\dot{m} = 0.25$ kg/s (water)
Undisturbed ground temperature	$\vartheta_g = 10.0$ °C

For a charging period of 24 h with 80 °C the simulation results of the fully discretized model (out, FEM) and the results of the Simulink EWS model (out,calc) are shown in Figure 5.2.2.

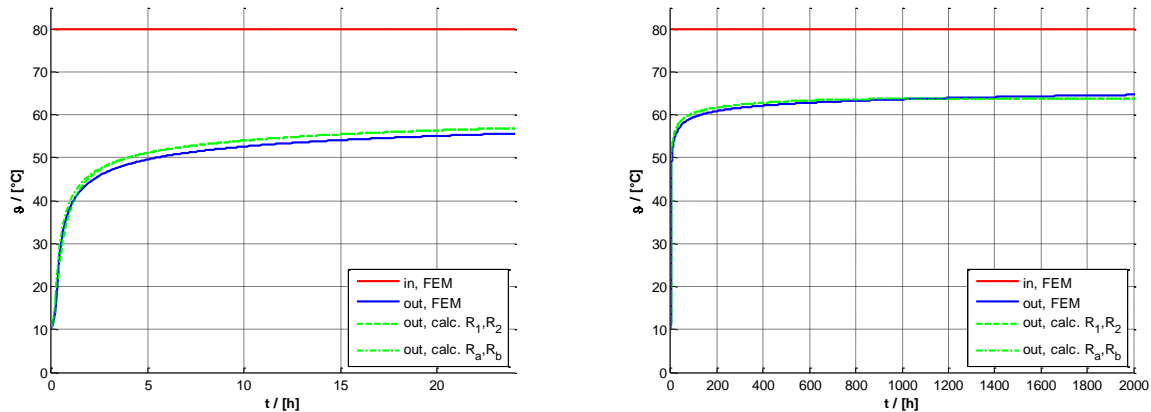


Figure 5.2.2 – Comparison of Simulink EWS model with ANSYS calculations (Bauer 2011), left first 24 h, right 2000 h

The agreement is relatively good with deviations of approx. 1 K after 24 h and a remaining deviation at the end of the simulation period, which may be a result of the simplified calculation of the resistances  $R_1$  and  $R_2$ . The dynamic behaviour (first 3 h) agrees quite well. The error with regard to energy (integrated power) is with about 3 % in 24 h acceptable, see Table 5.2.6.

Table 5.2.6 - Comparison of FEM results and EWS simulation results based on resistances  $R^1$ ,  $R^2$ .

	Q (2160h) [kWh]	Q (24 h) [kWh]
FEM	38138.7	715.2
EWS	38085.7	690.6
err / [%]	0.14	3.4

### Case 3: Long-term behaviour, comparison with EED and PHews

EED (earth energy designer) is considered as the reference tool for dimensioning of VGHX. PHews is the implementation of the EWS algorithms (with some minor simplifications) in the PHPP (Passive House Planning Package).

For the validation of the long-term behaviour typical loads of a single family passive house is applied, see Table 5.2.7. Profile 1 is a typical heating (H) load and profile 2 a load typical for heating and domestic hot water (DHW). The ground properties are summarized in Table 5.2.8 and borehole and heat exchanger parameters are listed in Table 5.2.9.

Table 5.2.7 – Load (heat extraction) in MWh, extraction power profile 1:  $P = 933$  W,  $Q = 1444$  kWh; profile 2:  $P = 1666$  W,  $Q = 5623$  kWh.

	Jan	Feb	Mar	Apr	May	Jun	Jul	Aug	Sep	Oct	Nov	Dec
Q (H)	0.43	0.21	0.09	0.03	0.00	0.00	0.00	0.00	0.00	0.03	0.22	0.43
Q(H+DHW)	1.24	0.65	0.36	0.25	0.26	0.25	0.21	0.21	0.25	0.26	0.50	1.19

Table 5.2.8 – Thermal properties of grout and ground.

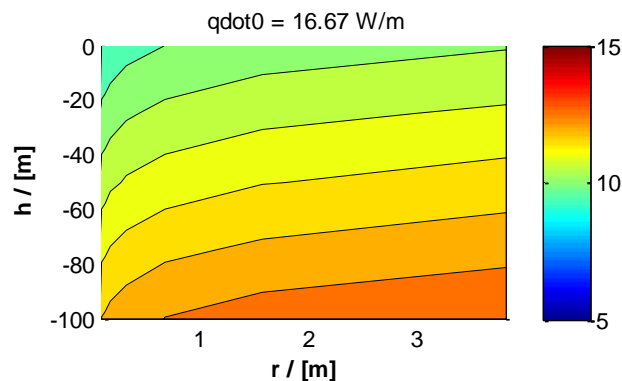
	Grout	Soil
$\lambda$ [W/(m K)]	1.0	2.0
$\rho$ [kg/m <sup>3</sup> ]	2000	2500
$c_p$ [J/(kg K)]	1000	800

Table 5.2.9 – Borehole and heat exchanger parameters.

Type	2U
Height	50 - 75 - 100 m
Borehole diameter	$D_b = 0.18$ m
Pipe	$D = 32/3.0$ mm
Pipe thermal conductivity	$\lambda_p = 0.48$ W/(m K)
Pipe distance	$Bu = 0.1293$ m
Mass flow	$\dot{m} = 0.5$ kg/s (water-glycol 25%)
Undisturbed ground temperature	$\vartheta_g = 10.0$ °C
Geothermal gradient	$T_{\text{Grad}} = 0.025$ K/m (= 0.05 W/m <sup>2</sup> )

The internal borehole resistance and the borehole thermal resistance are  $R_a = 0.46134$  (Km)/W and  $R_b = 0.11729$  (Km)/W.

As initial condition the temperature distribution for constant heat extraction of 50 years is calculated using peak extraction power. The resulting initial temperature field is shown in Figure 5.2.3.


 Figure 5.2.3 – Initial temperature distribution for a bore length of 100 m calculated for  $q = Q/H$ , with the peak extraction power  $Q$ .

The resulting temperature development for three different borehole lengths is shown in Figure 5.2.4 for the heating profile and in Figure 5.2.5 for the profile for heating and domestic hot water and is compared with EED and EWS simulation results.

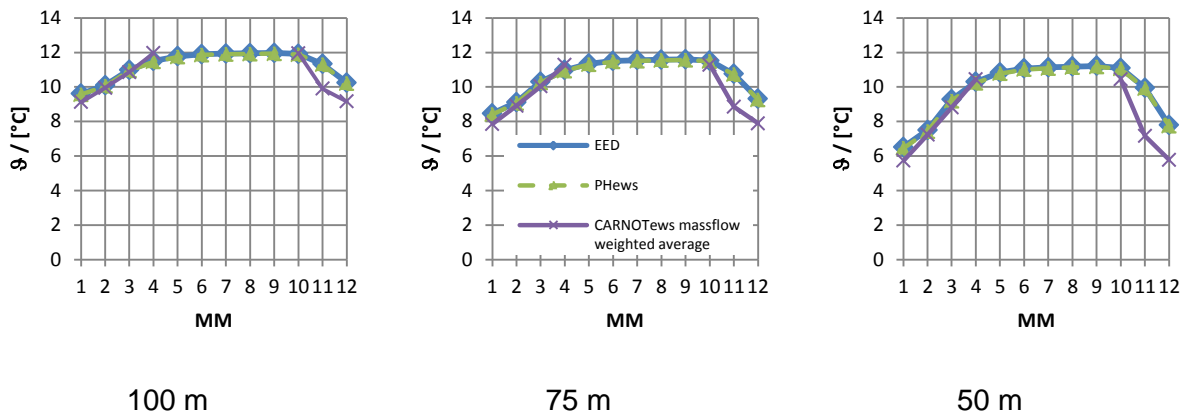


Figure 5.2.4– Temperature development for a 100 m (left), 75 m (centre) and 50 m (right) borehole, heating profile Q(H).

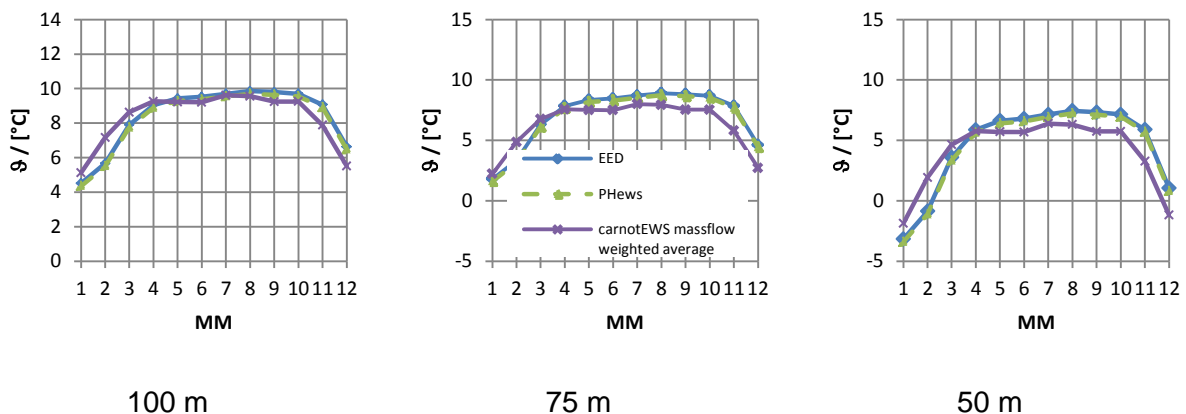


Figure 5.2.5– Temperature development for a 100 m (left), 75 m (centre) and 50 m (right) borehole, heating profile Q(H).

The agreement between EED and PHews is very good for all cases; the results of PHews are slightly more conservative. The development of the simulated temperature (carnotEWS) is comparable with the calculation results. However, as expected, the simulated monthly mass flow weighted temperatures are up 1 K to 2 K lower. The simulation yields more realistic results as actual extraction power and thus the respective borehole temperature is considered in each time step and not only the monthly energy balance as in the case of the calculation methods.

For a constant load of 12h per day with 1667 W the agreement between PHews and CARNOTews is very good as can be seen from Figure 5.2.6. Temperatures calculated with EED are slightly higher, in particular for higher specific loads.

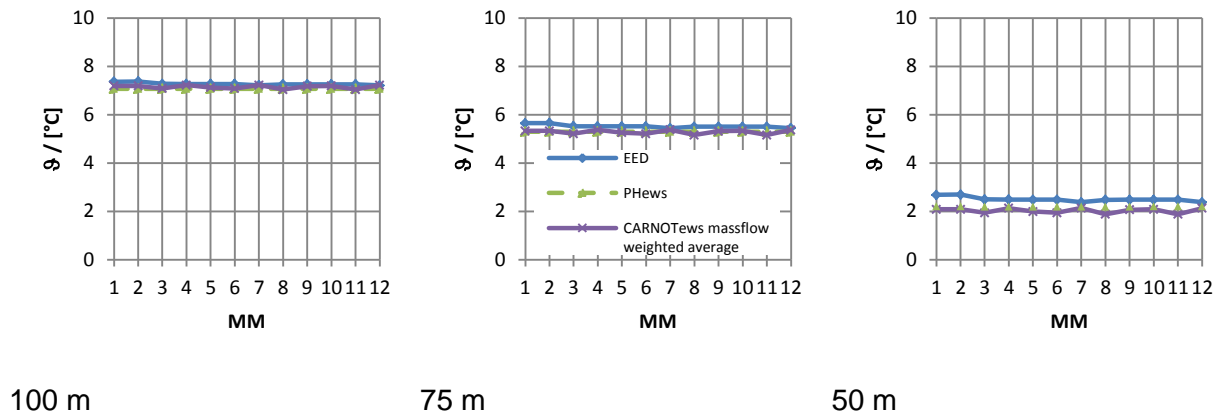


Figure 5.2.6 – Temperature development for a 100 m (left), 75 m (centre) and 50 m (right) borehole, constant extraction of 12 h per day with 1667 W.

### 5.3 Case Study: Passive House with building integrated HGHX

by Fabian Ochs

A horizontal ground heat exchanger that is installed in the blinding layer of the building represents a new cost effective concept. This system has already been realized in several passive houses and was investigated in detail in one house (Peper et al. 2010). The horizontal ground heat exchanger is thermally decoupled from the building by slab perimeter insulation, see Fig. 5.3.1.

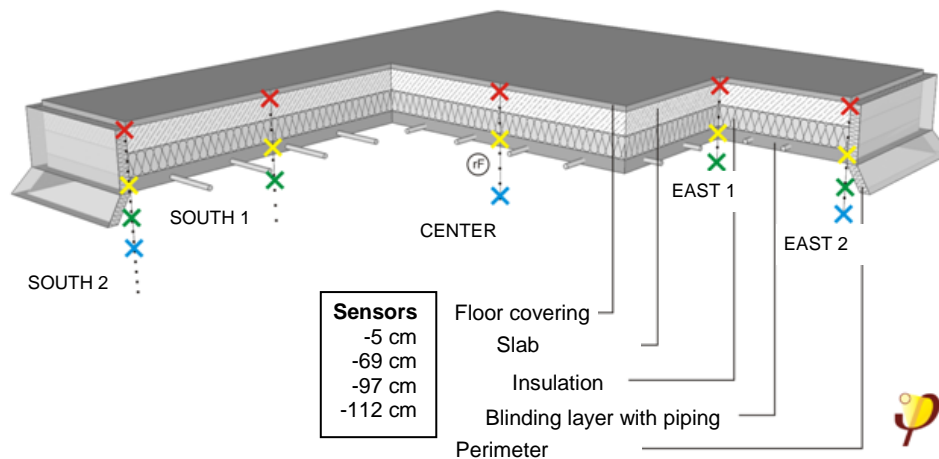


Figure 5.3.1 – Sketch of the horizontal ground heat exchanger in blinding layer with insulation skirt as well as position of temperature sensors below the building.

Compared to systems with vertical ground heat exchanger this concept is significantly more cost effective. However, as frost protection of the slab has to be guaranteed it works only with restrictions. Freezing of the ground can be prevented either by limiting the inlet temperature and thus the power of the heat pump or the operation time of the heat pump. Then an additional heat source would be required. Or the ground temperature can be increased by charging the soil with solar energy. A prerequisite for this concept is a highly insulated building envelope which ensures an extremely low heating consumption and the floor slab of the building must be insulated to a very high standard.

The detailed investigation of this building presented in Peper et al. (2010) has shown that this Passive House functions properly. The slightly higher heating consumption of 23 kWh/(m<sup>2</sup> a) can be partly explained with the fact that in spite of solar heat injection the ground under the floor slab is colder in winter than it would be without active heat withdrawal. This leads to an increased flow of heat into the soil (about 2 kWh/(m<sup>2</sup>a)), in spite of 300 mm of floor slab insulation. The indoor temperature in winter is apparently higher than the set temperature of the PHPP balance which is 20 °C (effect: 2.5 kWh/(m<sup>2</sup> a) per Kelvin of temperature increase). In addition, the heating consumption is increased compared to the calculations as at present the house is occupied by only two persons leading to lower specific internal heat gains (the building was planned as a two-family house with 152 m<sup>2</sup> treated floor area).

Only moderate temperatures of a maximum of 22 °C were measured in the ground below the building with almost no horizontal deviations, see Fig. 5.3.2. As could be shown by simulation, a larger solar collector area would only lead to slightly higher temperatures under the house, due to the comparatively rapid dissipation of heat in the ground. It is apparent that seasonal storage of surplus solar heat under the floor slab for the given dimensions of a single-family house is effective only to a limited degree. Hence, it is rather a system with solar regeneration of the ground as the source for the heat pump than seasonal storage.

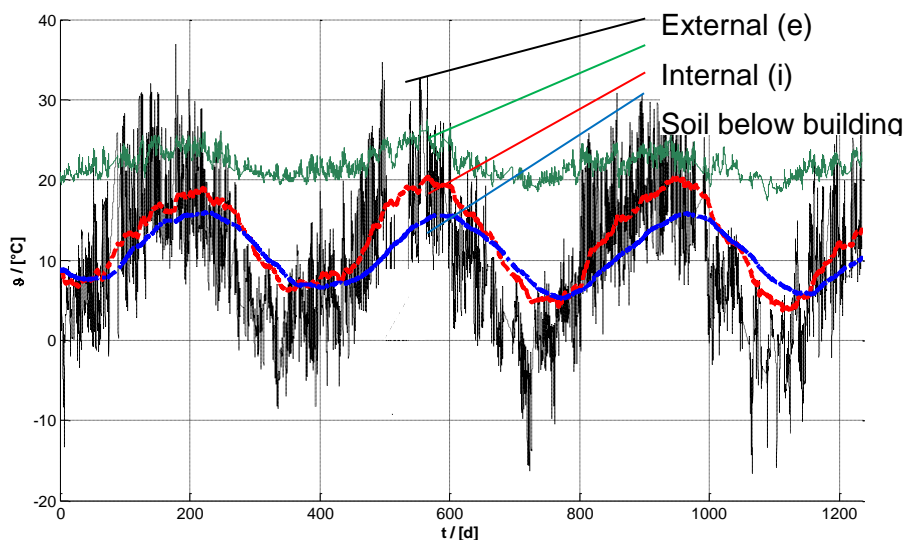


Figure 5.3.2 – Course of ambient temperature (e) internal temperature (i) ground temperature below the building (s) and undisturbed ground temperature (su).

The comparison between measured and simulated heat extraction and heat injection shows that the used 1D model predicts the behaviour with satisfying accuracy.

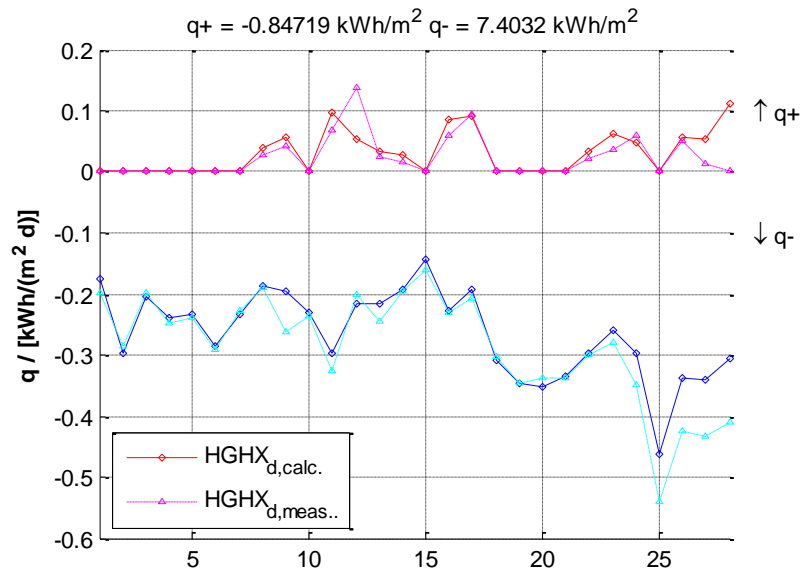


Figure 5.3.3 – Comparison of Simulink HGHX model with measurement data (Ochs et al. 2011), with heat extraction ( $q^-$ ) and heat injection ( $q^+$ ).

## 5.4 The top boundary of HGHX

by Fabian Ochs

For practical reasons, commonly a combined solar ambient temperature, which is calculated using climatic data, is applied as sole boundary condition with a combined convective and radiative heat transfer coefficient (3 type boundary condition).

Three approaches are compared: According to Eq. (5.4.1) to (5.4.3).

Eq. 5.4.1 PHPP 
$$\vartheta(t) = \vartheta_{amb}(t) + IK$$

Eq. 5.4.2 Glück (2009) 
$$\vartheta(t) = \vartheta_{amb}(t) + \frac{\alpha_s \cdot I}{h_e} + X \quad \text{with} \quad X = -3.9K$$

Eq. 5.4.3  
Nehring (in Glück) 
$$\vartheta(t) = \vartheta_{amb}(t) + \frac{\alpha_s \cdot I}{h_e} - \frac{\varepsilon \cdot \sigma_s}{h_e} \left( \left( \frac{T_{amb,m}}{100} \right)^4 + \beta \cdot (\vartheta_{amb}(t) - \vartheta_{amb,m}) \cdot (-e_{sky} \varepsilon_{sky} - e_{sur} \varepsilon_{sur}) \right)$$

with  $\alpha_s$  the absorption coefficient,  $h_e$  the heat transfer coefficient,  $\varepsilon$  the emission coefficient of the surface for long wave radiation,  $\sigma_s = 5.67 \text{ W}/(\text{m}^2\text{K}^4)$  the black body radiation coefficient,  $T_{amb,m}$  the daily average of the ambient air temperature,  $\beta \approx 1.05$  correction factor for linearization of radiative heat transfer,  $\varepsilon_{sky}$ ,  $\varepsilon_{sur}$  view factors ground-sky and ground-surrounding  $\varepsilon_{sky}$ ,  $\varepsilon_{sur}$  effective emission coefficient for ground-sky and ground-surrounding, respectively.

The approaches of the solar ambient temperature are compared with the exact solution (where absorption, convection and long wave radiation are calculated) taking climatic data of Strasbourg as an example (see Fig.5.4.1).

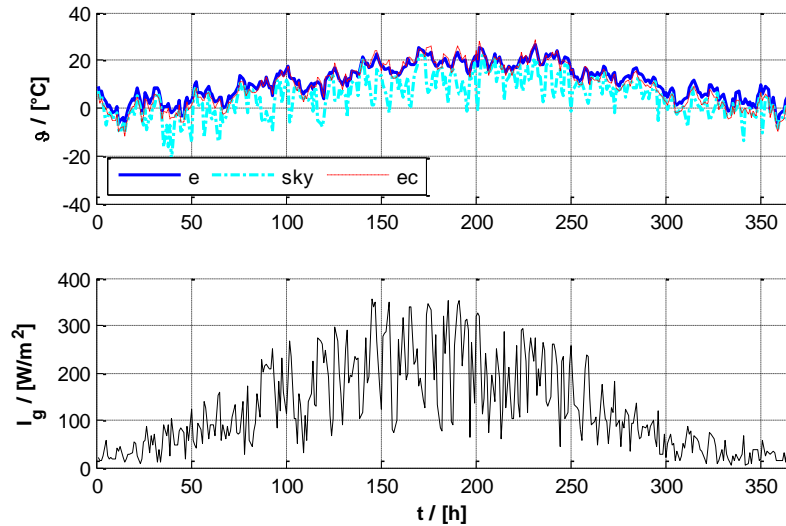


Figure 5.4.1 – Climatic data of ST, T44 (Meteonorm), e: external / ambient, sky: clear sky temperature, Jec: combined solar air temperature.

The combined solar air temperature approach has been compared with the exact solution at various depths. Results are presented in Fig.5.4.2.

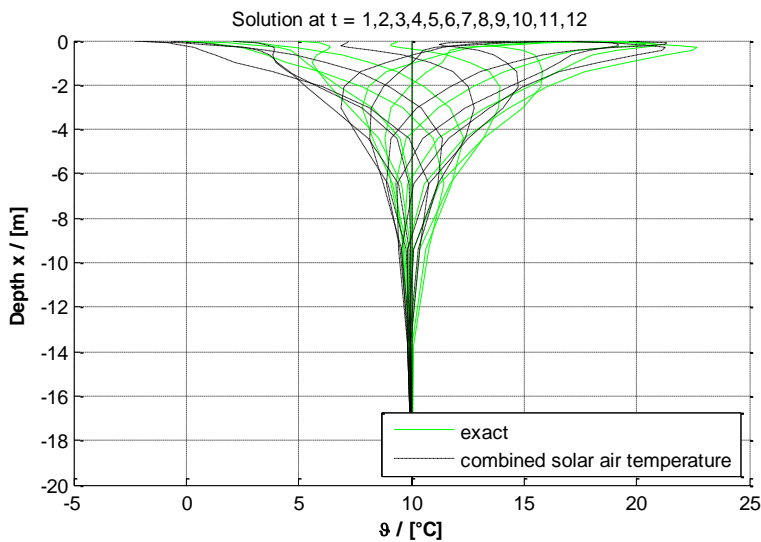


Figure 5.4.2 – temperature development as a function of depth for the exact calculation including convection, solar absorption and long wave radiation and for the combined solar air temperature (Jas).

The comparison between the three models (Eq. 5.4.1 to Eq. 5.4.3) against the exact solution is presented in Fig. 5.4.3. The simple approach using Eq. 5.4.1 gives a better match with the exact solution than the approach of the combined solar air temperature (Eq. 5.4.2 according to Glück) and is therefore recommended.

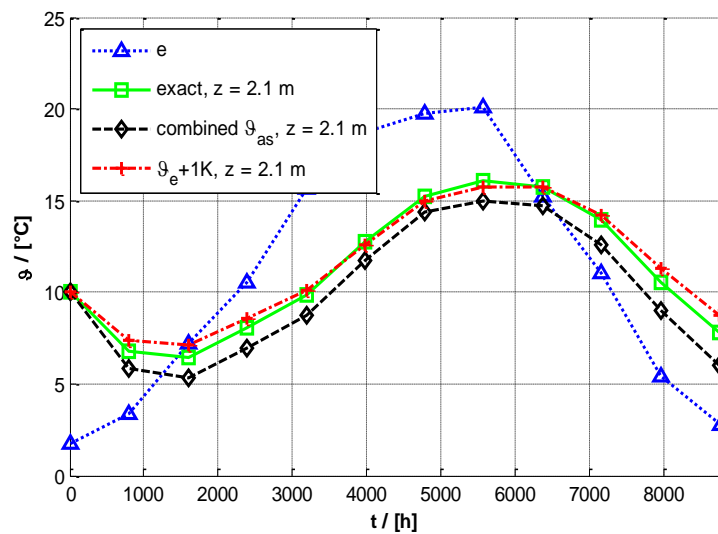


Figure 5.4.3 – Temperature in 2.1 m depth compared for different approaches for the solar ambient temperature calculated for climatic data of Strasbourg from (Meteonorm) for standard properties of the ground ( $\lambda = 2 \text{ W}/(\text{m K})$ ,  $\rho c_p = 2 \text{ MJ}/(\text{m}^3 \text{ K})$ ).

## 5.5 Short-term model validation and optimisation in TRNSYS

by Peter Pärtsch

Most of the GSHPs on the market are running with constant compressor speed leading to on-off operation in part load situations. Depending on the system design especially the integration concept of the heat storage the average running time of a heat pump lies in the range of about 10 min up to 1 hour. As described before the models SBM and DST models for TRNSYS are not applicable for that time scale as they neglect the fluid volume and the heat capacity of the GHX and the grout. On the other hand they allow simulating borehole fields. That is the reason why a short-term model validation and optimisation has been conducted.

First, the start-up behaviour of a VGHX at undisturbed ground temperature with a higher inlet temperature has been measured and analysed. Second, the experiment is simulated in TRNSYS with SBM, DST and EWS using the measured mass flow rate and the measured inlet temperature. Third, the models SBM and DST were optimised.

Fig 5.5.1 shows on the left side the measured inlet and outlet temperatures as well as the simulated outlet temperatures of SBM, DST and EWS. Obviously the SBM and the DST models deliver a steady-state result where the outlet temperature follows the inlet temperature with a constant difference. The deviation between measured and simulated injected heat of the whole 2 hour period is about -45 % (underestimation of the VGHX performance). In contrast the EWS model follows the measured outlet temperature with a high accuracy leading to a deviation -8 %.

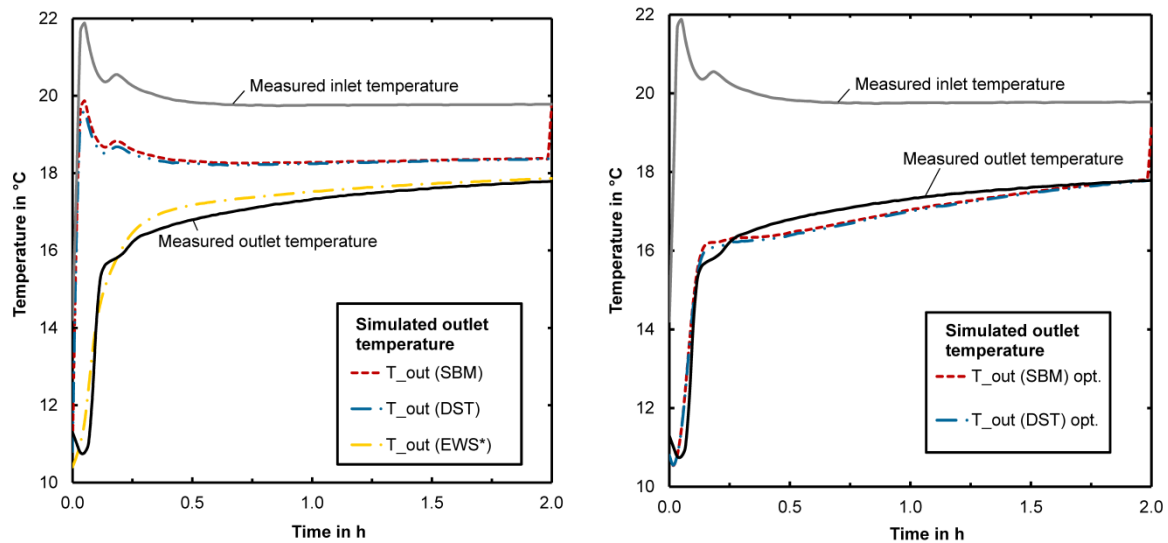


Figure 5.5.1 – Temperature in 2.1 m depth compared for different approaches for the solar ambient temperature from Pärish et al. (2013)

Pahud et al. (1996) describe that the borehole heat capacity can be considered using an adiabatic pipe model before the VGHX model in TRNSYS. But there is no description how to parameterize the pipe.

Here, a pipe model with wall capacity has been used. It has the same length as the VGHX. The inner and outer diameters of the pipe lead to the same volume of fluid and grout and the same material properties are used. Fig. 5.5.1 on the right side shows the improvement of SBM and DST. Now, the deviation of the injected heat is reduced to +5 % for SBM and +10 % for DST respectively. It is shown in Pärish et al. (2013) that even a 3D-COMSOL simulation doesn't approximate better because of the parameter uncertainties of the VGHX.

In order to “discharge” the heat capacity of the pipe in phases without heat extraction or injection the pipe and the VGHX are connected with a bypass. The error of a typical system simulation (single family house, heat demand 45 kWh/(m<sup>2</sup>·a), Strasbourg, DHW-storage, heat pump directly to the floor heating, with or without solar ground regeneration) is shown in Fig. 5.5.2 from Bertram et al. (2013).

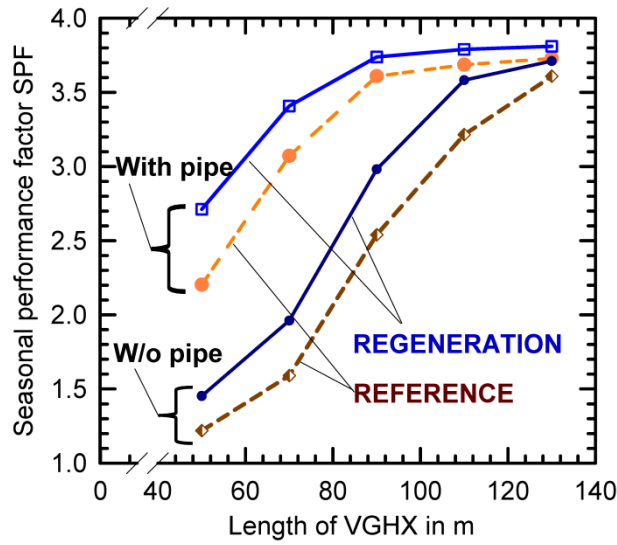


Figure 5.5.2 –Effect of the model optimisation (with or without pipe) on the SPF of a SFH45 simulated with DST, from Bertram et al. (2013)

Obviously a correct transient behaviour of the VGHX model is very important for the system efficiency with or without solar ground regeneration. Dimensioning tools like EED which use steady-state models or monthly averaged loads tend to oversize the VGHX. This leads to higher investment costs and to a small improvement of the efficiency.

## Bibliography

- Bauer D., 2012. Zur thermischen Modellierung von Erdwärmesonden und Erdsonden-Wärmespeichern, Ph.D. Thesis, ITW, Uni Stuttgart.
- Bennet, J., Claesson, J. And Hellstrom G., 1987. Multipole method to compute the conductive heat transfer to and between pipes in a composite cylinder. Notes on heat transfer 3-1987. Department of Building Physics, Lund Institute of Technology, Lund, Sweden.
- Bernier, M. Pinel, P., Labib, R. and Paillot, R., 2004. A multiple load aggregation for annual hourly simulations of GCHP systems. HVAC&R Research 10 (4), pp. 471-487.
- Bertram E. Pärish P. Tepe R., 2013. Solare Wärmepumpensysteme mit Erdwärmesonden - Konzeptvergleiche, Proceedings of the 12. Internationale Anwenderforum Oberflächennahe Geothermie, Neumarkt i. d. Opf., Germany, OTTI e. V., Regensburg, Germany.
- Bi Y., Chen L., Wu C., 2002. Ground heat exchanger temperature distribution analysis and experimental verification, Applied Thermal Engineering, Volume 22, Issue 2, pp. 183–189.
- Bianchi M. A., 2006. Adaptive modellbasierte prädiktive Regelung einer Kleinwärmepumenanlage Diss. ETH No. 16892.
- Bojic, M., Trifunovic, N., Papadakis, G. & Kyritsis, S., 1997. Numerical simulation, technical and economic evaluation of air-to-earth heat exchanger coupled to a building. Energy, 22(12), pp. 1151-1158.
- CANMET, 2002. Commercial Earth Energy Systems: A buyer's guide. CANMET Energy Technology Centre, Natural Resources of Canada.
- Carbonell, D., Cadafalch, J., and Consul, R., 2011. A transient model for radiant heating and cooling terminal heat exchangers Applied to Radiant Floors and Ceiling Panels. Proceedings of ISES Solar World Congress, Kassel, Germany.
- Carslaw, H.C. and Jaeger, J.C., 1947. Conduction of heat in solids, Oxford, U.K., Clarendon Press.
- Cauret O., Bernier, M., 2009. Experimental validation of an underground compact collector model, Effstock, Stockholm.
- Claesson, J, Javed, S, 2011. An analytical method to calculate borehole fluid temperatures for time-scales from minutes to decades. ASHRAE Transactions, vol. 117(2), pp. 279-288.
- Claesson, J. and Eskilson, P., 1987. Conductive heat extraction by a deep borehole, analytical studies. Tech. Rep., Lund University, Sweden.
- Esen, H., Inalli, M. & Esen, M., 2007. Numerical and experimental analysis of a horizontal ground-coupled heat pump system. Building and Environment, 42(3), pp. 1126-1134.
- Eskilson, P., 1986. Superposition Borehole Model. Manual for Computer Code. Department of Mathematical Physics, Lund Institute of Technology, Lund, Sweden.
- Eskilson, P., 1987. Thermal analysis of heat extraction boreholes. PhD Thesis, Lund University, Department of Mathematical Physics, Lund, Sweden.
- Feist W., 1999. Arbeitskreis kostengünstige Passivhäuser, Protokollband Nr. 17, Dimensionierung von Lüftungsanlagen in Passivhäusern, Darmstadt.

- Florides, G. & Kalogirou, S., 2007. Ground heat exchangers--A review of systems, models and applications. *Renewable Energy*, 32(15), pp. 2461-2478.
- Giardina, J.J., 1995. Evaluation of Ground Coupled Heat Pumps for the State of Wisconsin. University of Wisconsin.
- Glück, B., 2009. Simulationsmodell "Erdwärmekollektor" zur wärmetechnischen Beurteilung von Wärmequellen, Wärmesenken und Wärme-/Kältespeichern.
- Hellstrom, G. & Sanner, B, 1997. EED- Earth Energy Designer User's Manual, Version 1.0. Prof. Dr. Knoblich & Partner GmbH, Wezlar, Germany.
- Hellstrom, G., 1991. Ground Heat Storage - Thermal Analysis of Duct Storage Systems. Part I Theory, Lund University, Department of Mathematical Physics, University of Lund, Sweden.
- Hollmuller, P. & Lachal, B., 2001. Cooling and preheating with buried pipe systems: monitoring, simulation and economic aspects. *Energy and Buildings*, 33(5), pp. 509-518.
- Huber, A. & Pahud, D., 1999. Erweiterung des Programms EWS für Erdwärmesondenfelder. Im Auftrag des Bundesamtes für Energie, Zürich.
- Huber, A. & Schuler, O., 1997. Berechnungsmodul für Erdwärmesonden. Im Auftrag des Bundesamtes für Energiewirtschaft, Zürich.
- IGSHPA, 1988. Closed-Loop/ground-Source Heat Pump Systems - Installation Guide, International Ground-Source Heat Pump Association, Oklahoma State University, Stillwater, Oklahoma, USA.
- Ingersoll, L.R., Plass, H.J. & Ingersoll, A.C., 1954. Heat conduction with engineering, geological and other applications. New York, Mc Graw-Hill.
- Javed, S, Claesson, J, 2011. New analytical and numerical solutions for the short-term analysis of vertical ground heat exchangers. *ASHRAE Transactions*, vol. 117(1), pp. 3-12.
- Kavanaugh, S.P. & Rafferty, K., 1997. Ground-source heat pumps. Design of geothermal systems for commercial and institutional buildings, American Society of Heating Refrigerating and Air-Conditioning Engineers, Inc., Atlanta.
- Lamarche, L. & Beauchamp, B.A, 2007a. A new contribution to the finite line-source model for geothermal boreholes. *Energy and Buildings*, 39, pp. 188-198.
- Lamarche, L. & Beauchamp, B.A, 2007b. New solutions for the short-time analysis of geothermal vertical boreholes. *International Journal of Heat and Mass Transfer*, 50, pp. 1408-1419.
- Lamarche, L., 2011. Analytical g-function for inclined boreholes in ground-source heat pump systems, 40, pp. 241-249.
- Lamarche, L., Stanislaw, K. and Beauchamp, B.A, 2010. A review of methods to evaluate borehole thermal resistance in geothermal heat-pump systems. *Geothermics*, 39, pp. 187-200.
- Li, Z. & Zheng, M., 2009. Development of a numerical model for the simulation of vertical U-tube ground heat exchangers. *Applied Thermal Engineering*, 29(5-6).
- Marcotte D. & Pasquier, P., 2008. Fast fluid ground temperature computation for geothermal ground-loop heat exchanger system. *Geothermics*, 37, pp. 651-665.

- Mei, V.C., 1986. Horizontal ground-coil heat exchanger theoretical and experimental analysis. Oak Ridge National Laboratory, TN (USA).
- Mihalakakou G., Santamouris M., Asimakopoulos D., 1994. Modelling the thermal performance of earth-to-air heat exchangers, J. Solar Energy, vol. 53, pp. 301-305.
- Muraya, N.K., O'Neal, D.L. and Heffington W.M., 1996. Thermal interference of adjacent legs in a vertical U-tube heat exchanger for ground-coupled heat pump. ASHRAE Transactions 102(2), pp. 12-21.
- Ochs F., Feist W., 2012a Experimental Results and Simulation of Ground Heat Exchangers for a Solar and Heat Pump System for a Passive House, Innostock, Lleida.
- Ochs F., Peper S., Schnieders J., Pfluger R., Bianchi Janetti M., Feist W., 2011. Monitoring and Simulation of a Passive House with innovative Solar Heat Pump System, ISES Solar World Congress, Kassel.
- Ochs, F. Feist, W. 2012b FE Erdreich-Wärmeübertrager Model Für Dynamische Gebäude- und Anlagensimulation mit Matlab/Simulinkm, Bausim, Berlin.
- Pärisch, P. Mercker, O. Oberdorfer, P. Bertram E. Tepe R. Rockendorf G., 2013. Optimization of TRNSYS models for borehole heat exchangers regarding the combination with solar heat, Proceedings of the 12. Internationale Anwenderforum Oberflächennahe Geothermie, Neumarkt i. d. Opf., Germany, OTTI e. V., Regensburg, Germany.
- Pahud, D., 2012. The Superposition Borehole Model for TRNSYS 16 or 17 (TRNSBM). User Manual for the April 2012 Version. Internal Report. ISAAC - DACD- SUPSI, Switzerland.
- Pahud, D., Fromentin, A. & Hadorn, J.-C., 1996. The Superposition Borehole Model for TRNSYS (TRNSBM). User Manual for the November 1996 Version. Internal Report. LASEN - DGC- EPFL, Switzerland.
- Paul, N.D., 1996. The effect of grout thermal conductivity on vertical geothermal heat exchanger design and performance. Msc. Thesis South Dakota University, Vermillion, SD, USA.
- Peper, S.; Schnieders, J.; Ochs, F., Feist, W., 2010. Messtechnische Untersuchung und wissenschaftliche Auswertung zur saisonalen Wärmespeicherung über Sole-Register unter der Bodenplatte eines Passivhauses mit Dämmschürze Abschlussbericht, Forschungsvorhaben Aktenzeichen: Z 6 – 10.08.18.7-06.19. / II2-F20-06-013, im Auftrag des BBR, Darmstadt.
- Piechowski, M., 1999. Heat and Mass Transfer Model of a Ground Heat Exchanger, Theoretical Development. Int. J. Energy Research.
- Ramming, K, 2007. Bewertung und Optimierung oberflächennaher Erdwärmekollektoren für verschiedene Lastfälle. PhD Thesis, TU Dresden, Dresden, Germany.
- Rawlings, R, 1999. Ground source heat pumps. A technology review. A BSRIA Technical note, TN 18/1999.
- Sharqawy, M.H., Mokheimer, E.M. and Badr, H.M., 2009. Effective pipe-to-bore thermal resistance from vertical ground heat exchangers. Geothermics 38, pp. 271-277.
- Spitler, J.D., 2000. A design tool for commercial building ground loop heat exchanger. In Proceedings of the 4th International Conference off Heat Pumps in Cold climates, Asylmer, QC, Canada, August 2001, 17-18, pp. 1-16.
- TESS 2006 TESS Libraries V2.0 Documentation, Thermal Energy System Specialists.

- Thornton, J.W., Mc Dowell, T.P., Shonder, J.A., Hughes, P.J., Pahud, D. Hellstrom, G., 1997. Residential vertical geothermal heat pump systems models. Calibration to data. ASHRAE Transactions 103 (2): pp. 660-674.
- Tzaferis, A., Liparakis, D., Santamouris, M. & Argiriou, A., 1992. Analysis of the accuracy and sensitivity of eight models to predict the performance of earth-to-air heat exchangers. Energy and Buildings, 18(1), p.35–43.
- Wetter M. and Huber A, 1997. Vertical Borehole Heat Exchanger EWS Model, Model description and implementing into TRNSYS.
- Wu Y, Gan G., Gonzalez R. G., Verhoef A., Vidale P. L., 2011. Prediction of the thermal performance of horizontal-coupled ground-source heat exchangers, International Journal of Low-Carbon Technologies Advance Access published July 13.
- Wu, Y., 2010. Experimental measurement and numerical simulation of horizontal-coupled slinky ground source heat exchangers, Applied Thermal Engineering 30 (2010) 2574e258.
- Yavuzturk, C. and Spitler, J.D., 1999. A short time step response factor model for vertical ground loop heat exchangers. ASHRAE Transactions, 105(2): pp. 475-485.
- Zeng, H., Diao, N. and Fang, Z., 2002. A finite-source model for boreholes in geothermal heat exchangers. Heat Transfer - Asian Research 31 (7), pp. 558-567.

## Appendix A – GHX Models Table

### Verticle GHX

Name/ID	Platform(s)	Type of HX			heat conduction solution		boundary assumptions				special effects				special	Literature		
		pip	2U	GHX fields	far-field	near field	top	bot	side	grdProp variable	ice	lhor	rain	Vgw				
DST Type 557	TRNSYS	-	√	√									-		-		Hellström 1989	
EWS Type 451	TRNSYS			√		ILS	1D FD	param	inf	inf	with depth		-	dTavg	-		Wetter & Huber 1997, Huber & Schuler 1997	
DSTP Type 280	TRNSYS	?	√	√	√	3D FD	1D FD	param	inf	inf	with depth		-	-	-	yes	a) b)	Pahud et al. 1996, Hellström 1989
SBM Type 281	TRNSYS	?	√	√	√	3D FD	1D FD	param	inf	inf	no		-	-	-	no	b)	Pahud 2012, Eskilson 1986
PILESIM2	stand-alone	?	√	√	√	3D FD	1D FD	param	inf	inf	with depth		-	-	-	yes	a) b)	Pahud 2007
EED	stand-alone	?	√	√	√	g (FLS)	anal	const	inf	inf	no		-	-	-	no		Hellström and Sanner 2000
EWS	stand-alone		√	√	√	g (FLS)	1D FD	param	inf	inf	with depth		-	dTavg	-			Huber & Pahud 1999
EWS	Polysun			√	√	g (FLS)	1D FD	param	inf	inf	with depth		-	dTavg	-			Huber & Pahud 1999
EWS	Simulink		√	√	√	g (FLS)	1D FD	param	inf	inf	with depth		-	dTavg	-			Bianchi 2006, Ochs 2012

Type of HX: pip: pipe-in-pipe tube, 2U = double U-tube

heat conduction solution: ILS: infinite line source theory, g (FLS): g-Functions based on the finite line source theory, anal: analytical solution, 1D FD: 1D finite difference model

Nodes: Number of nodes in different directions: l: nodes along the length of the pipe, h: horizontal, v: vertical, a: axisymmetric, r: radial

boundary assumptions: param: input parameter (temperature), const: const. temperature at ground surface, inf: const. temperature at an infinite distance.

a) influence of ground water flow computed using important simplifications – not validated

b) the influence of solar radiation can be integrated as a correction in the evolution of the input temperature at the ground surface

## Horizontal GHX

Name/ID	Platform(s)	Type of collector			Nodes					boundary assumptions				special effects				special comments	Literature	
		HP	B	T	l	h	v	a	r	top	bottom	side	grdProp variable	ice	lhor	rain	Vgw			
TRN Type 556 / ORNL model	TRNSYS	√	-	-	-	N	-	-	N	N	t(tau)	tgrd(tau)	tgrd(tau)	no	-	-	-	-		Mei 1986, Giardina 1995
Glück	stand-alone	√	-	-	-	1	N	N	-	-	t(tau)	tgrd = const	adiabatic	with depth	√	√	-	-		Glück 2009
TRN Type 981	TRNSYS	√	-	-	-	1	N	N	-	-	t(tau)	tgrd = input	adiabatic	with depth	√	√	-	-		Glück 2009, Haller 2011
Ramming	TRNSYS	√	-	-	-	1	N	N	-	-	t = input	???	???	with depth and time	√	√	√	-		Ramming 2007
TRN Type 460	TRNSYS	√				N	N	N	-	-	t(tau), Q(tau), adiabatic	t(tau), Q(tau), adiabatic	t(tau), Q(tau), adiabatic	variable in 3D	-	-	-	-	a)	Hollmuller and Lachal 1998
Simulink 1D	Simulink	√	-	-	-	1	N	-	-	-	t(tau)	tgrd(tau)	-	with depth	√	√	-	-		Ochs 2011
Simulink 2D	Simulink	√	√	√	√	1	FEM				t(tau)	tgrd(tau) adiabatic	adiabatic	variable in 2D	√	√	-	-		Ochs 2012b

Type of collector: HP: horizontal pipes, B: basket, T: trench

Type of model: p: physical

Nodes: Number of nodes in different directions: l: nodes along the length of the pipe, h: horizontal, v: vertical, a: axisymmetric, r: radial

boundary assumptions: t(tau): temperature as a function of time, Q(tau): heat flux as a function of time, adiab.: adiabatic, tgrd: temperature of the (undisturbed) ground, grdProp variable: variable properties of the ground at different depths.

special effects: ice: influence of ice formation, lhor: radiative surface gains, rain: influence of rain, Vgw: influence of ground water flow.

a) hypocaust / sensible and latent heat transfer of moist air in an earth duct

### Literature

Giardina, J.J., 1995. Evaluation of Ground Coupled Heat Pumps for the State of Wisconsin. Master Thesis, UNIVERSITY OF WISCONSIN.

Glück, B., 2009. SIMULATIONSMODELL "ERDWÄRMEKOLLEKTOR" zur wärmetechnischen Beurteilung von Wärmequellen, Wärmesenken und Wärme-/Kältespeichern. Rud. Otto Meyer-Umwelt-Stiftung, Hamburg.

Eskilson, P., 1986. Superposition Borehole Model. Manual for Computer Code. Department of Mathematical Physics, Lund Institute of Technology, Lund, Sweden.

Hellström, G., 1989. Duct ground heat storage model - Manual for Computer Code. Department of Mathematical Physics, University of Lund, Sweden.

Hellström, G. & Sanner, B., 2000. Earth Energy Designer, User's Manual, version 2.0 (<http://www.buildingphysics.com/>).

Hollmuller, P. & Lachal, B., 1998. TRNSYS compatible moist air hypocaust model. Final report, Centre universitaire d'études des problèmes de l'énergie, Genève.

Huber, A. & Schuler, O., 1997. Berechnungsmodul für Erdwärmesonden. Bundesamt für Energiewirtschaft, Bern.

Huber, A. & Pahud, D., 1999. Erweiterung des Programms EWS für Erdwärmesondenfelder. Bundesamt für Energie, Bern.

- Mei, V.C. & Emerson, C.J., 1985. New approach for analysis of ground-coil design for applied heat pump systems. In: ASHRAE Trans., American Society of Heating, Refrigeration and Air Conditioning Engineers, 91, 1216 - 1224.
- Mei, V.C., 1986. Horizontal ground-coil heat exchanger theoretical and experimental analysis. Oak Ridge National Laboratory, TN (USA).
- Pahud, D., 2007. PILESIM2: Simulation Tool for Heating/Cooling Systems with Energy Piles or multiple Borehole Heat Exchangers. User Manual. ISAAC – DACD – SUPSI, Switzerland.
- Pahud, D., 2012. The Superposition Borehole Model for TRNSYS 16 or 17 (TRNSBM). User Manual for the April 2012 Version. Internal Report. ISAAC - DACD- SUPSI, Switzerland.
- Pahud, D., Fromentin, A. & Hadorn, J.-C., 1996. The Duct Ground Heat Storage Model (DST) for TRNSYS Used for the Simulation of Heat Exchanger Piles. User Manual, December 1996 Version. Internal Report. LASEN - DGC- EPFL, Switzerland
- Ramming, K., 2007. Bewertung und Optimierung oberflächennaher Erdwärmekollektoren für verschiedene Lastfälle. PhD Thesis, TU Dresden, Dresden, Germany.
- von Cube, H.L., Ludwig, E., Sattlegger, J. & Rohde, J., 1980. Erarbeitung eines Optimierungsverfahrens für die Auslegung von Erdbodenrohrschlangen als Wärmequelle für Wärmepumpen. Report BMFT - FB - T 80-121, Bundesministerium für Forschung und Technologie, Karlsruhe.
- Wetter, M. & Huber, A., 1997. TRNSYS Type 451 - Vertical Borehole Heat Exchanger EWS Model Version 2.4. Zentralschweizerisches Technikum Luzern & Huber Energietechnik.